positive for HSV-1/2 and 2/13 (15.4%) positive for VZV in the skin, and 5/20 (25%) cases positive for polyoma virus in the kidney. In none of the cases without VCPE did a positive finding by IHC result in significant changes in clinical care.
Conclusions: The vast majority of cases for which IHC is ordered for viral infections are negative. A positive IHC stain without diagnostic VCPE is most common for CMV in the GI tract. However, this result rarely impacts patient treatment. These findings suggest that IHC for viral infections without a high degree of clinical or histologic suspicion is unnecessary in the vast majority of cases.

1545 Interpretation of HSV Positive Respiratory Specimens Using Quantitative PCR

Christopher Suciu, Michelle Stram, Jansen Seheult, Charles R Rinaldo. University of Pittsburgh Medical Center, Pittsburgh, PA.
Background: Oropharyngeal reactivation of Herpes Simplex Virus Type 1 (HSV1) is widely recognized to occur in immunosuppressed and critically ill patients. However, it is highly contentious whether the identification of HSV in the lower respiratory tract represents innocuous distal shedding or a true pneumonitis requiring treatment.
Design: The laboratory database was queried for viral cultures conducted between 1/1/14-8/31/15 at a large academic institution with a significant transplant population. HSV positive respiratory viral culture specimens were collected from the archives for HSV genotyping and viral copy number quantification. The published threshold of $>10^5$ copies/ml was considered to be indicative of a clinically significant respiratory viral load. The bronchoscopic findings and associated cytology during specimen collection were reviewed. The medical records of HSV positive patients were evaluated to determine immune status, ICU admission, therapeutic management, and mortality.
Results: 5931 lower respiratory tract viral cultures were conducted, with positive HSV1 viral culture in 46 specimens from 40 patients. PCR results were obtained on 41 specimens from 37 patients. Mean viral copy number was higher in samples collected from ICU vs non-ICU patients ($1x10^7$ vs $1x10^6$, $p<0.05$). There was no statistically significant relationship with mortality or immune status. Diagnostic bronchoscopy and cytology had low sensitivity (36%, 18.8%). Viral cultures had a poor turnaround time (average 10.1 d, range 2-31 d), which diminished their clinical relevance.

Table 1. Bronchoscopy and Cytology Correlation with Viral Count

	+ Bronchoscopy[A]	+ BAL Cytology[B]
Above Threshold (Viral copy $>10^5$)	9/25 (36%)	3/16 (18.8%)
Below Threshold (Viral copy $<10^{[illegible],5}$)	4/9 (44.4%)	0/7 (0%)

A. Viral inclusions or cytopathic effect observed

B. Mucosal ulceration, friability, or edema

Table 2. Immune Status, ICU Admission, Mortality, and Viral Count

	Above Threshold (Viral count > $1x10^{[illegible],5}$ï»¿)	Average Viral Copy #
Immunocompromised	69.5% (16/23)	$2.13x10^6$
Immunocompetent	86.3% (15/18)	$1.45x10^7$
ICU	88.5% (23/26)	$1.13x10^7$
Non-ICU	53.3% (8/15)	$1.08x10^{[illegible],6}$
Death during hospital admission	86.7% (13/15)	$8.93x10^{[illegible],6}$
Survival to discharge	69.2% (18/26)	$6.76x10^{[illegible],6}$

Conclusions: This is the largest US based study using quantitative PCR to evaluate the clinicopathologic significance of HSV isolated from the lower respiratory tract. Quantitative PCR is a specific, sensitive, and rapid test that provides better data for clinicians to treat their patients.

1546 Histopathologic Features of T. Pallidum Infection Differ between the Rectum and Anus

Julie Y Tse, Vikram Deshpande, Judith A Ferry, Lawrence Zukerberg. Massachusetts General Hospital, Boston, MA.
Background: Syphilis is a sexually transmitted disease, caused by Treponema pallidum, which has become increasingly prevalent. Syphilis not uncommonly manifests in the gastrointestinal (GI) tract, either as a primary or secondary manifestation, but may be overlooked either clinically or histopathologically. Endoscopic lesions of GI syphilis are non-specific, and may consistent of ulcers, fissures, and polypoid masses, which can be mistaken for inflammatory or neoplastic conditions. The classic histopathology of a lymphoplasmacytic infiltrate in the lamina propria may not be reliable. In order for the prompt treatment of GI syphilis and prevention of long-term complications, it is important for the pathologist to consider and recognize this entity. We aimed to evaluate the histopathologic manifestation of GI syphilis to improve diagnostic accuracy.
Design: The surgical pathology file at the Massachusetts General Hospital was searched for cases of syphilitic or treponemal infection of the GI tract. Hematoxylin and eosin slides were evaluated, as was immunohistochemistry (IHC) for T. pallidum. We evaluated and compared the histopathologic features of GI syphilis by site (rectum versus anus).
Results: Three cases of GI syphilis were available for review (distal colon n=2; anus n=1). Patients were male, ages 33 to 52. Review of the clinical data and histopathology was performed. Clinical evidence of syphilis was confirmed by serology. The endoscopic appearance of lesions included ulceration, nodularity, and fissures, with differential diagnoses including inflammatory bowel disease and lymphoma. Histopathologic review revealed that while the classically described pattern of a dense lymphoplasmacytic infiltrate with granulomatous inflammation was seen in the anus, the rectal cases had a dense lymphohistiocytic infiltrate with frequent eosinophils. Features of inflammatory bowel disease were not identified. Abundant spirochetes were identified in the mucosa by T. pallidum IHC in all cases.
Conclusions: The prevalence of syphilis is on the rise, but manifestation in the GI tract may be overlooked due to its nonspecific clinical and histopathologic features. We studied the histopathologic features of GI syphilis, and found an inflammatory response in the rectum that differed from that seen in the anus. We wish to highlight these differences to increase awareness and to provide the pathologist with morphologic clues for this entity.

1547 Evolution of High-Risk Human Papillomavirus Genotypes in Anal Biopsies from HIV-Positive Patients after Long-Term Follow-Up

Hai Wang, Yiang Hui, M Ruhul Quddus, Jayasimha N Murthy, Zakaria Grada, Dongfang Yang, C James Sung, Shaolei Lu, Li Juan Wang. Warren Alpert Medical School of Brown University, Providence, RI.
Background: Human immunodeficiency virus (HIV)-positive patients are often infected with multiple high-risk human papillomavirus (HR-HPV) genotypes. Multiple HR-HPV infections are associated with development of anal intraepithelial neoplasia (AIN) and squamous cell carcinoma (SCC). While HR-HPV genotypes in HIV-positive adults may change after one year of follow-up, differences in HR-HPV types after longer periods are unknown. We sought to compare genotypes on initial and long-term follow-up anal biopsies from HIV-positive patients to assess factors that may influence their HR-HPV status and risk of developing AIN or SCC.
Design: Institutional records from 1985-2015 were reviewed to identify HIV-positive patients with 2 consecutive anal biopsies obtained at least 5 years apart. Demographics and potential risk factors were collected. Representative lesional tissue was dissected from unstained tissue sections for each case. DNA was extracted and HR-HPV genotyping for 14 types was performed using multiplex PCR followed by signature Tag/Capture probe hybridization. The initial and follow-up genotyping results were compared using Student's two-tailed t-test.
Results: Fifteen HIV-positive patients each with anal biopsies taken at least 5 years apart (mean=9.3 years) were identified, 12 of which had both initial and follow-up tissue available for genotyping. Among the 25 biopsies collected, 12 (48%) were high-grade AIN, 9 (36%) were low-grade AIN or condylomas, and 4 (16%) were SCC. In these biopsies, 76% contained non-HPV 16 and 18 types. Genotyping revealed that one patient was HR-HPV negative on both biopsies. Among the 11 patients positive for HR-HPV, genotype profiles changed from initial to follow-up biopsy in all patients. The mean number of HR-HPV types decreased from 2.8 on initial biopsy to 1.4 at follow-up (p=0.011), but multiple types were detected in 54.5% (6/11) at follow-up.
Conclusions: In the first long-term follow-up study of HR-HPV in anal lesions from HIV-positive patients, we found that in all patients positive for HR-HPV, the genotypes present differed between initial biopsy and follow-up. Most of these lesions contain non-HPV 16 and 18 types which may not be prevented by vaccination. Despite a reduction in number of HR-HPV types at follow-up, the majority of patients still had multi-type infections. Our findings suggest that there is wide temporal variation of HR-HPV genotypes in HIV-positive patients which may contribute to the high risk of developing AIN or SCC in this population.

Informatics

1548 Assessment of Workload Measures in Anatomic Pathology

Gareth W Bryson. Queen Elizabeth University Hospital, Glasgow, United Kingdom.
Background: Measuring workload in anatomic pathology is a perennial problem because of the large variation of specimen types which require vastly different amounts of time to analyse and report. Systems which have been employed include counting Request, Specimen or Slide numbers and more complex systems including Medicare Relative Value Units (RVU's) and Royal College of Pathologists (RCPath) Workload Points. With increasing sub-specialisation it is essential to find a fair and reliable measure of Workload across sub-specialty Teams to ensure that each of these sections is appropriately resourced.
Design: In our institution Adult Anatomic Pathology and Cytology Requests are prospectively scored at Accessioning and given a RCPath Workload Score and a Local Workload Score using a Modified RCPath Scoring System (which includes more specimen 'bundling' and point caps per Request). Work is distributed in our Department according to the Local Workload Score. A test set of 20,000 consecutive requests was identified and numbers of Specimens, Blocks and Slides were ascertained. These requests were retrospectively scored for Medicare RVU's.
Consultant Pathologists in the department (n=34) were surveyed and asked to score how reasonable their measured workload was per hour on a sliding scale (with 100% being appropriate, <100% being too little work and >100% being too much work). A separate survey could be completed for each team.
These data were analysed by Team and used to calculate a mean appropriate Local Workload Points per unit time. This was then combined with the test set to calculate the appropriate number of Specimens, Slides, RCPath Points and RVU's per Hour.

Results: A total of 52 survey responses were received. Analysis showed that the variation in appropriate score per unit time was lowest for the Local Workload Points (Standard Deviation – Local Points, 0.41; Specimens, 1.34; RVU's, 1.46; Requests, 1.54; RCPath Points 2.08; Slides, 4.19).
Conclusions: Statistical analysis confirmed that the variance was lower for the Local Workload Points than for other commonly employed workload measures. They provide a useful measure of workload which Consultants across all sub-specialty teams felt was a fair refection of work per unit time. In comparison, RCPath Workload Points, Medicare RVU's, or Specimen, Block or Slide numbers show more variation in score per unit time across Teams, making them less useful for determining appropriate distribution of resource in an Anatomic Pathology Department.

1549 An Independent, Variant-Level Assessment Exposes Gaps in Probe Design and Coverage in Sequencing-Based EGFR Testing

Michelle Call, Sushama Thakker, Charlie Kim, Glenda Anderson. Farsight Genome Systems, Sunnyvale, CA.
Background: EGFR inhibitors play an important role in the treatment of lung cancers with specific variants known to induce sensitivity or resistance to these targeted therapies. FDA-approved labels require testing for EGFR exon 19 deletions and exon 21 (L858R). The 2013 consensus guideline published by AMP, CAP and IASLC, and endorsed by ASCO, has expanded this list to 26 EGFR variants, on exons 18, 19, 20, and 21 recommended for routine testing in lung adenocarcinomas (2013 Lindeman). Sequencing is often used in EGFR variant detection, but the method is sufficiently sensitive only if the processing protocol provides adequate coverage or read depth at the location where the variant is to be detected.
We set out to assess whether the target enrichment protocols used in sequencing-based testing provide consistent and adequate coverage at each of the 26 EGFR variant locations. To perform this assessment, we built a novel algorithm, *CoverageFx,* capable of computing and reporting read depth at each location, for each sample.
Design: Data from 12 experiments, conducted by 11 different laboratories were chosen from published sources. Inclusion criteria were EGFR included in the target enrichment design and average coverage greater than 100x. The data includes Illumina and Ion sequencers and target enrichment from Agilent, Illumina, Ion and Raindance. Patient samples included were from 10 different cancer types including lung, colon, breast, and melanoma. 3-5 samples were selected from each experiment, for a total of 55 samples analyzed by the *CoverageFx* algorithm.
Results: The EGFR exon 19 variant region was consistently assessed at sufficient read depth across 100% of the experiments. This is not surprising, as exon 19 deletions are activating mutations included in early trials and the labels of the first approved EGFR inhibitors. By contrast, EGFR variants in exon 21 (including L858) were measured at sufficient read depth in only 58% of the experiments and exons 18 and 20 in 42%. Significant sample-specific coverage variation was found in the colon, gastric and bladder tumor samples.
Conclusions: This study demonstrates that average coverage is an inadequate, even misleading, quality measure in clinical sequencing. Laboratories using sequencing-based test panels should confirm adequacy of coverage at each reportable genomic region when validating the laboratory developed test. Ideally, coverage adequacy should be evaluated with each reportable sample.

1550 Machine Learning to Predict Successful Hematopoietic Progenitor Cell Collection from the Sysmex XN3000 Blood Analysis Data

German Campuzano-Zuluaga, Cesar A Llanos, Joseph Zeitouni, Artur Rangel-Filho. University of Miami Health System, Miami, FL.
Background: Hematopoietic progenitor cell (HPC) apheresis (HPCA) is the preferred source of HPCs for transplantation. Predicting the target CD34-ISHAGE count before a HPCA procedure can help the involved laboratories allocate resources. We propose that characterization of blood cell populations, measured by hematology analyzers, can be used to train a set of models to predict collection target success.
Design: Retrospective data from donors was obtained. CD34 counts were performed by flow cytometry. Pre-procedure CBCs were obtained using a Sysmex XN3000 analyzer. The response variable was defined as whether a target was achieved or not (range 2–6 CD34-ISHAGE). All analyzer variables, age, gender and collection day were considered (total 83). Data was split into training (80%) and validation sets. The final set of features included those that showed a significant difference ($p<0.1$) by the dichotomized CD34-ISHAGE. For each target level, 4 algorithms were parallel-trained and the output predicted probabilities were used as input for a logistic regression stacked model. Preprocessing included scaling, centering and principal component analysis. 10-fold cross-validation was performed. Model performance was assessed by accuracy.
Results: HPCA and CBC data were obtained for 64 collections (33 patients; training = 52). A final set of 10 features was used for training (WBC, neutrophil, lymphocyte, immature granulocyte, monocyte, basophil, platelet, and NRBC counts, and neutrophil and NRBC %). All models showed similar good accuracy in the training and validation sets. The staked models showed significant improvement over the individual models and the validation accuracy showed good agreement with the training results (Tab 1).

Tab 1. Accuracy (%).

Target	RRF	SVM	RLR	RBF	Stacked	Validation
2	78	70	73	74	91	83
3	80	82	81	82	92	50
4	83	82	85	80	94	58
5	84	84	85	82	98	67
6	85	85	85	82	98	75

Conclusions: Increase in HPCs is associated with significant hematologic changes that can be used to assess the probability success for a given HPCA. Combining these cellular features via a stacked prediction model showed good accuracy to predict the target success for a HPCA. This approach offers a cheap alternative to CD34 flow cytometry. A larger sample size could improve help improve the precision of the prediction framework which should be validated and tested in an independent sample.

1551 Functional Validation of MicroRNA Activity Inferred by ActMiR in Bladder Cancer

Mireia Castillo-Martin, Ana Collazo Lorduy, EunJee Lee, Jun Zhu, Carlos Cordon-Cardo. Icahn School of Medicine at Mount Sinai, New York, NY.
Background: MicroRNAs (miRs) play a key role in cancer, both in tumorigenesis and tumor progression. In the past years, miR expression signatures have been reported as prognostic biomarkers in different tumor types including bladder cancer (BC). However, miR's expression does not always correlate with activity. We recently developed a novel computational method, named ActMiR, for explicitly inferring the activity of miRs based on the changes in expression levels of target genes. The main objective of this study was to validate the inferred miRs' activity using BC as a model.
Design: We applied ActMiR in 405 BC cases from The Cancer Genome Atlas (TCGA) database for which information from both mRNA and miR expression was available. Different BC cell lines (5637 and HT1376 for basal BC, SW780 and HT1197 for p53-like BC, and RT4 and RT112 for luminal BC) as well as the immortalized urothelial cell line [Human Urothelium cell (HUC)] were used to perform the *in vitro* functional validation. RNA was extracted from these cells basally and after inhibition of miR106-5p with specific anti-miR inhibitor (Taqman, Life Technologies); miR and target genes' expression was assessed by qRT-PCR.
Results: ActMir analyses revealed that a subset of 306 out of 1044 miRNAs were differentially expressed between tumor and normal samples at p-value$<10^{-4}$. More importantly, at p-value$<10^{-4}$, 155 out of 556 miRNAs were functionally active. From these, only four (miR106b, miR532, mir556, and mir134) were significantly differentially expressed, functionally active and showed prognostic significance. We chose to further analyze mir106b because it showed the biggest and most significant difference in activity between normal and cancer cells (p-value$<2*10^{-11}$). As inferred by ActMir, mir106-5p was significantly overexpressed in all cancer cells when compared to HUC. Basal cells showed the highest fold increase (mean of 39; range: 31-47), followed by luminal (mean of 19; range: 5-32) and p53-like cells (mean of 8; range: 3-13). Inhibition of mir106b-5p was performed to assess whether the predicted target genes were consequently upregulated.
Conclusions: Our results underscore the value of ActMir for inferring miR activity in BC from a systems biology perspective. It endorses ActMir as a promising tool for studying casual effects of miR activity on target genes, and ultimately for determining survival outcomes of BC patients.

1552 Development of a Cloud-Based Histology Database for Collaborative Cancer Research

Ke Cheng. HistoWiz Inc, Brooklyn, NY; SUNY Downstate Medical Center, Brooklyn, NY.
Background: The development of Whole Slide Imaging (WSI) technology has allowed for the digitization of histology data, but there is a pressing need to build a scalable and cost-effective IT infrastructure to archive and manage the multi-terabyte databases for archiving and data sharing. Development of a virtual slide database on a scalable IT infrastructure will improve histology data viewing and searching resulting in enhanced global scientific collaboration, allowing *cancer to be fought cooperatively instead of individually*.
Design: The main repository for WizBase is a relational database powered by Amazon Web Services with online viewing, collaboration and long-term archiving of WSIs. We will also create ontology parameters and tagging approach using 3 types metadata: Type I, classification parameters--specimen information and experimental details captured at order submission; Type II, ontology terms--annotation added upon visualization of the slide by HistoWiz and slide owners; and Type III, crowdsourced tags and collaborative comments not requiring formality or standardization.
Results: We have developed a robust IT infrastructure allowing for viewing, tagging and searching of histology images. HistoWiz viewer is the first Cloud based viewer that allows users to instantly view their histology slides on any mobile device without the need to download any files, software or plug-ins.

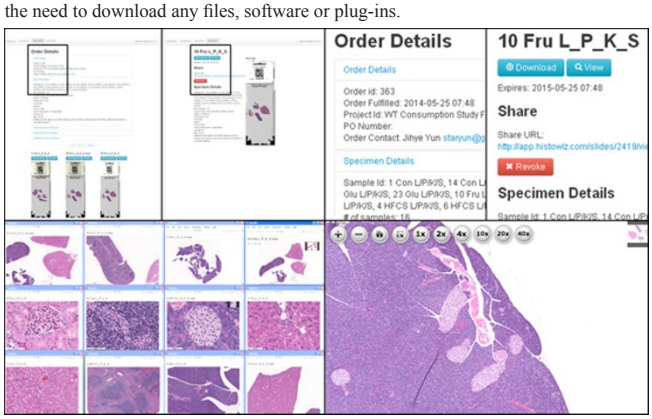

Furthermore, we have establish ontology parameters for the classification and tagging of digital pathology cancer images, and slide metadata are captured during online order submission. Finally, through defined field and free-text tagging of the slide metadata, users can search for slides meeting specific criteria. Searches based on similarity to a particular subject slide metadata allows ranking slide relevancy. The crowdsourced database currently has >10,000 histology slides and is growing at a rate of 300% per year.
Conclusions: WizBase™ is the first centralized Cloud-based WSI database for cancer histopathology with an image-tagging web application to facilitate histology-driven data mining. WizBase™ can be regarded as the scientific hybrid of a microscopy product with the viewing power of Google Earth combined with the search and crowd-sourcing of Flickr.

1553 A Web-Based Platform-Independent Whole Slide Imaging Education Suite for Pathology Didactics

Paul Christensen, Nathan Lee, Suzanne Z Powell, Michael J Thrall, Patricia Chevez-Barrios. Houston Methodist Hospital, Houston, TX.

Background: Unknown conferences are common in pathology training. Prior to conferences trainees preview case slides and then static histology images are presented while they discuss their differential diagnoses (DDx). This approach has no mechanism to collect residents' DDx, no innate archival mechanism, and provides no metrics about how trainees previewed each case. Our institution developed a vendor-neutral, web-based whole-slide image (WSI) education suite to address these deficiencies.
Design: Over 3 weeks we surveyed user experiences with 3 different WSI viewing systems (Ventana Virtuoso, Jviewer, Google Maps), then combined original code with open source projects to create a custom web-based maps-style WSI viewing system. We installed a server (1000 USD) on the hospital intranet. We scanned slides at 20-40x (iScan Coreo, Ventana Medical Systems) for our weekly conference and incorporated a survey into which users entered their training level and Ddx for each case. Using server log files we captured where users looked in the case and recorded bandwidth usage.
Results: There were 17 conferences and 163 cases over 74 days. 142 unique computers (UC) viewed the cases with an average of 17 UC/conference. The system required a mean network throughput of 421 KB/s (peak: 2310 KB/s - 8123 KB/s). Users reported the web-based maps-style viewer as easiest to use and with minimal latency. Users recognized digital pathology as a safe alternative to light microscopy in didactic settings, but the majority did not agree that digital pathology was equivalent to light microscopy in clinical practice. Heat maps of user viewing experiences were successfully created.

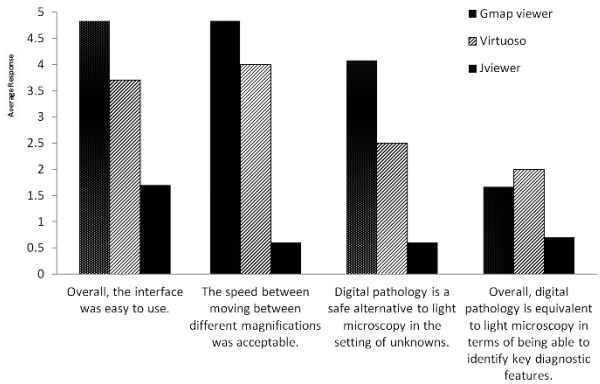

Figure 1a. User reported opinions about different WSI viewers

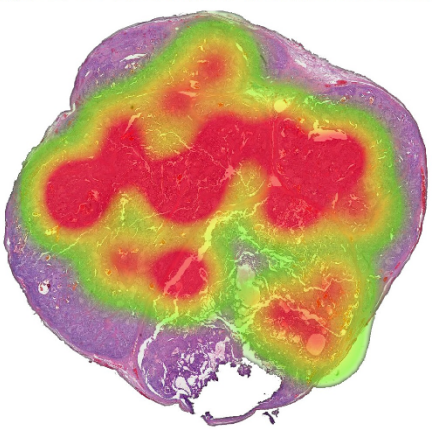

Figure 1b. Trainee composite heatmap. Papillary thyroid carcinoma, cribriform-morular variant

Conclusions: This is the first web-based, platform-independent education suite that integrates WSI with a survey to collect pre-conference Ddx. This allows the presenter to analyze submitted Ddx to tailor didactic sessions around group-specific deficiencies. Cases are archived and easily accessed for post-conference review. We can create heat map visualizations without eye tracking equipment or software. Network and server requirements to support multiple simultaneous users are low. Future work is centered on collecting board-review cases, creating review modules, and generating novel viewing pattern visualizations.

1554 HCV Genie V 2.0: A Web 2.0 Interpretation and Analytics Platform for the Versant Hepatitis C Virus (HCV) Genotype Line Probe Assay

Alex Dussaq, Abha Soni, Christopher D Willey, Seung L Park, Shuko Harada. UAB, Birmingham, AL; Community Health Systems, Franklin, TN.

Background: Hepatitis C virus (HCV) genotyping at our institution is performed using the Versant Hepatitis C virus genotype 2.0 Line Probe Assay (LiPA). The last step of this procedure is a manual, time-consuming, error prone process that involves the comparison of bands on a test strip to a physical reference table. A resident, working under the supervision of a molecular diagnostician and a pathology informaticist, had developed an HCV genotype interpretation platform that identifies the strain of HCV based on the banding. However, identifying bands on the strip was done manually. This study serves as a follow-up with an MD/PhD student porting this system to an open web environment and adding an analytical step utilizing a scanned LiPA image to generate the genotyping results.
Design: Using a pure web environment (JavaScript [JS], HTML5, CSS), the student (a) ported the original, clinically validated, HCV genotype interpretation program, "HCV Genie," from PHP to JS, (b) created image analysis algorithms that convert LiPA images into band calls, and (c) built a user interface to utilize these tools. This was done utilizing JS to allow the analysis to be done without the data ever leaving the investigator's computer, eliminating any potential data privacy concerns. Additionally, results of the analysis are downloadable as both machine readable JavaScript Object Notation (JSON), and a printable human readable report.
Results: The original HCV Genie was written, deployed, clinically validated, and proven to be identical to human expert interpretation (n = 200) over the course of 2 weeks. It decreased the time needed to interpret results by 53% for residents, but results among experienced lab technicians were more equivocal. Since the most time-consuming part is to identify each band on the strip, HCV-Genie V2 allows us to further minimize analysis time and eliminate errors, thereby, increasing the quality of patient care.
Conclusions: Our original program provided results that are identical to the manual workflow, but (a) with reduced manual steps and (b) in a timeframe similar to that of the most well-trained manual interpreter, regardless of the program user's experience level. This iteration focused on developing lane and band detection algorithms, and creating a publically available tool that eliminates data privacy concerns. Future iterations of this program will focus on allowing users to store and aggregate results in a database of their choosing, allowing for advanced data analytics of HCV genotypes.

1555 Machine-Readable, Structured Pathology Report Data: A Requirement for Pathologists' Computer Assisted Diagnosis (pCAD) in Breast Cancer Signout

Jeffrey L Fine, Michelle Heayn, Navid Farahani. University of Pittsburgh School of Medicine, Pittsburgh, PA.

Background: Pathologists' Computer Assisted Diagnosis (pCAD) is a hypothetical, intelligent system that is intended to focus pathologist attention on expert decisions while automating other tasks. For example, tumor measurement requires pathologist expertise, but size and T-stage data entry could be handled automatically. Instead of pathologists driving microscopes, pCAD systems would interactively chauffeur pathologists to diagnostic areas in whole slide images (WSIs), then automatically construct a report. In addition to sophisticated image analysis, this would also require total access to laboratory information system (LIS) data. Structured pathology data has previously been explored, but this project focused on a novel, unmet need: workflow automation (pCAD) using machine-readable reports in the setting of breast cancer.
Design: Breast cancer biopsy and mastectomy pathology reports (from de-identified data) were created in XML format (eXtensible Markup Language), including structured gross description and histology data. Referencing a pre-existing, simple pCAD mockup, maps of data flow were created. Simulated examples of customized pathology reports were created for different audiences (e.g. oncologist, patient, primary care provider, surgeon, etc.). Creation of mockups (e.g. the customized reports) is a well-established software design strategy that permits a complex system to be rapidly modeled then explored for usability.
Results: The structured XML data and maps were complex but modeled information requirements for pCAD signout of breast cancer resections. These include data from the core biopsy (diagnosis, prognostic stain results) and from the resulting resection (gross description and histology). The model included pCAD outputs, such as auto-annotated WSIs and auto-generated report data. The simulated, customized pathology reports were very different from one another despite conveying similar information, albeit to different audiences (e.g. patient, clinician, primary care team).
Conclusions: Real automation of signout work would be revolutionary. Pathologists could be freed of non-expert tasks, to focus on providing better patient care to the health care team. Machine-readable pCAD data allows pricision-targeted reports that appear superior to a one-size-fits-all approach. Finally, automation may create opportunities for expanded value-add pathologist activities (e.g. direct patient interaction, greater availability to clinicians).
Reference: FINE JL. 21st Century Workflow: A proposal. J Pathol Inform 2014, 5:44.

1556 Image Recognition: Orientation and Visual Field Bias in Digital Pathology

Sharon E Fox, Richard S Vander Heide, Charles Law, Beverly E Faulkner-Jones. LSU Health Sciences Center, New Orleans, LA; Boston Children's Hospital, Boston, MA; Kitware, Inc., Clifton Park, NY; Beth Israel Deaconess Medical Center, Boston, MA.

Background: Digital pathology has been demonstrated as a useful tool for both clinical diagnosis and education. In order to optimize digital platforms, it is important to understand the visual process by which pathologists arrive at image-based diagnoses. We hypothesize that this process represents a gain of adult visual expertise – a phenomenon

that has been linked to configural image interpretation rather than recognition of specific individual features. The current study examines this form of visual expertise during diagnosis, and extends these findings to the use of digital pathology in the clinical setting.
Design: Pathologists and trainees were recruited to view a variety of digital pathology media, including whole-slide images (WSIs), and multi-image viewers, with varying specimen orientation. We used a Philips UFS whole slide scanner for the creation of WSIs, and hosted the scans on https://slide-atlas.org, a high-performance web-based digital pathology system. Participants explored the images in each format and rendered a diagnosis. For a subset of images, participants were instructed to assess a diagnostic feature within the image. A Tobii X2-60 eyetracker was used to collect gaze pattern data throughout the experiment. Eye-tracking data and slide movement were analyzed and compared across image categories.
Results: Gaze patterns during diagnostic exploration of digital media demonstrated that initial fixations were clustered on the left side of the specimen image, regardless of media type or image orientation ($p<0.05$). Furthermore, a greater number of saccades occurred towards the left side of the image during diagnosis. Trainees with less than one year of anatomic pathology experience did not demonstrate this laterality effect for images in an "inverted" orientation. The laterality effect was not present when participants were asked to assess a specific diagnostic feature within the image.
Conclusions: The development of gaze patterns for rapid assessment and categorization is common to many forms of acquired visual expertise. Our studies suggest that the diagnostic process is a form of expertise akin to that which is developed for human face recognition, with similar visual biases. These findings enhance our understanding of the image-based diagnostic process, and have important implications for the improvement of digital media and computer-assisted diagnosis.

1557 Digital Pathology and Anatomic Pathology Laboratory Information System Integration Supports Digital Surgical Pathology Sign-Out

Huazhang Guo, Douglas J Hartman, Jonhan Ho, Anthony L Piccoli, Matthew O'Leary, Jeffrey McHugh, Joe Birsa, Mark Nyman, Curtis Stratman, Jeffrey L Fine, Samuel A Yousem, Liron Pantanowitz. University of Pittsburgh Medical Center, Pittsburgh, PA.
Background: Transformation to digital pathology may offer benefits over labor-intensive, time-consuming and error-prone manual processes. However, because most workflow and lab transactions are centered around the Anatomical Pathology Laboratory Information System (APLIS), digital workflow adoption ideally requires integration with the APLIS. A Digital Pathology System (DPS) was recently implemented at our institution for future primary diagnosis. We demonstrate how back-end integration with this DPS and our APLIS supports a digital workflow to sign-out surgical pathology cases.
Design: Pathology cases were accessioned into the APLIS (CoPath Plus, Cerner). Glass slides from these cases were then digitized (Omnyx VL120 scanner), in a core histology laboratory, and uploaded into the DPS (Omnyx IDP). The APLIS sends key case data to the DPS via a Publishing Web Service. The DPS matches scanned images with the correct case using barcode labels on slides and information received from the APLIS. When pathologists at remote locations open a case in the DPS, additional case information is retrieved from the APLIS through a Query Web Service.
Results: Following validation of the aforementioned integration, 8 pathologists tested signing out more than 150 surgical pathology cases. APLIS-DPS integration enabled pathologists to review digital slides on one monitor, while simultaneously viewing pertinent case metadata such as clinical information, gross pathology findings, and prior case details. This digital workflow eliminated the need for manually matching slides to cases or to continuously reference the relevant data in the APLIS. Also, pathologists avoided having to wait for glass slides to be delivered.
Conclusions: DPS-APLIS integration was instrumental for successfully implementing a digital solution at our institution for surgical pathology sign-out. This integration enhanced our digital workflow, diminished the potential for human error related to matching, and improved the sign-out experience for pathologists.

1558 Digital Image Analysis Reliably Estimates Bone Marrow Trephine Biopsy Cellularity

Ashley S Hagiya, Ali Etman, Imran N Siddiqi, Russell K Brynes, Mohamed E Salama. Keck School of Medicine, University of Southern California, Los Angeles, CA; University of Utah, Salt Lake City, UT.
Background: Evaluation of cellularity is an essential component of bone marrow trephine biopsy examination. Results are usually expressed as visual estimates (VE) of percent marrow surface area. Cellularity is nearly 100% at birth and drops to 40-60% after puberty. Digital image analysis (DIA) offers the promise of more accurate and objective measurements of all components of the trephine biopsy. We correlated VE cellularity with DIA, and assessed age-related changes.
Design: One-hundred fifty-one adult bone marrow samples without evidence of malignancy in the marrow were assessed for cellularity by VE to the nearest 10% by three hematopathologists, and the median value determined. Sections were scanned using an Aperio AT2 Scan-scope and analyzed for marrow surface area using a Cytonuclear (version 1.4) algorithm on HALO software. Results were expressed as percent hematopoietic cell area (HC) [HC/HC+fat]. A subset of patients with normal to minimally abnormal CBCs (mild anemia), were assessed for age related changes.
Results: Cellularity determined by VE and DIA demonstrated a strong Pearson's correlation ($r=0.88$, $p<0.001$, Figure 1).

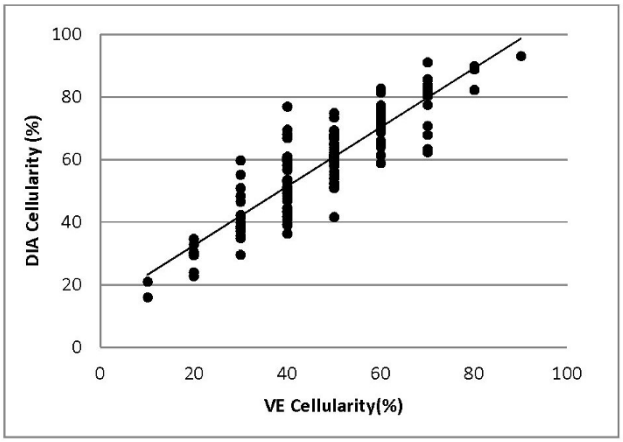

Bland-Altman analysis correlating the mean of VE and DIA cellularity with the difference between the VE and DIA cellularity detected a negative trend (data not included). Mean cellularities by DIA were plotted according to age, and fell within the conventional reference range (40-60%) across all age groups (Figure 2).

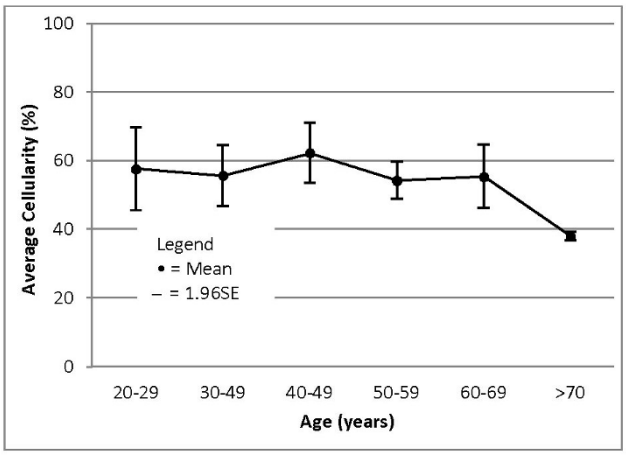

Conclusions: Cellularity assessed by VE and DIA showed strong correlation. The average cellularities fell within the normal range (40-60%) for all age groups. When comparing the differences between VE and DIA cellularity, there was either an overestimation by DIA or underestimation by VE. This may indicate that VE is affected by perception bias.

1559 Live Remote Digital Microscopy in Peripheral Smear Evaluation: Validation and Intraobserver Variability

Diana M Haninger, Mehdi Nassiri, Elizabeth D Settembre, Shanxiang Zhang, Jiehao Zhou. Indiana University School of Medicine, Indianapolis, IN.
Background: Peripheral blood smear (PBS) review is a routine laboratory activity which requires pathologist review when abnormal indices, atypical cells, or critical findings, such as blasts, are identified. Prompt, accurate evaluation is essential and real-time remote digital microscopy (DM) can facilitate rapid review when a pathologist is not physically present, such as at remote laboratories or after hours/weekends. Here, for purposes of validation and assessment of utility, we evaluate intraobserver concordance/discrepancy of PBS evaluation with glass slides (GS) and DM using VisionTek M6 robotic digital microscopy and TeamViewer imaging software.
Design: 12 PBS flagged for review along with CBC data and brief clinical histories were de-identified and independently viewed by 5 reviewers (3 hematopathologists, 2 fellows). Slides were loaded on a VisionTekM6 robotic microscope at an outside laboratory and viewed remotely using TeamViewer software. Reviewers recorded impression, imaging quality(0-3), confidence of interpretation(0-3), minutes required for interpretation, device used(desktop/laptop computer), location(laboratory/home), and connection type(wireless/Ethernet). Slides were then viewed using light microscopy and results for impression, minutes to interpretation, and confidence of interpretation were recorded.
Results: The intraobserver concordance between GS and DM was 92%, with 5 discordant interpretations. There were 2 instances of blasts noted on DM but not GS (2 separate patients), 1 instance of blasts noted on GS but not DM, and 2 instances of plasma cells noted on GS but not DM (same patient). The 3 discrepancies involving blasts involved 1 reviewer, and the 2 remaining discrepancies involved 2 reviewers. Technical problems with DM consisted mainly of errors with the auto-focus feature on the VisionTek software as well as contrast issues on specific slides and difficulty assessing nuclear texture and granularity. DM required an average of 6 minutes to interpret with overall confidence of 2.5/3; GS required an average of 2.3 minutes with overall confidence of 2.9/3.

Conclusions: While the overall time required for evaluation on DM was nearly 3 times that of GS review, and overall confidence level for DM was slightly lower than GS, there was a high level of intraobserver concordance between DM and GS. The technical problems encountered with DM were of minimal significance in the overall confidence level and ease of diagnosis. DM can be a useful methodology when in-house pathologist review of PBS may not be feasible.

1560 Can Polarizable Material Be Identified from Automatically Acquired Digital Slides?

Douglas J Hartman, Morgan Jessup, Simon Watkins, Liron Pantanowitz. University of Pittsburgh Medical Center, Pittsburgh, PA; University of Pittsburgh School of Medicine, Pittsburgh, PA.

Background: Historically, pathologists have utilized polarizers with light microscopy in order to view polarizable material within their glass slides. With the advent of whole slide imaging, the ability to perform this polarization has not been incorporated into standard whole slide imaging scanners. Remotely, viewing digital slides without the ability to perform polarization if needed is a limiting factor of this technology.

Design: For this proof of concept study, we collected glass slides of amyloid (H&E, Congo red stain), crystals (gout, pseudogout, calcium oxalate) and foreign-body granulomas (suture, silicone). Brightfield imaging was performed with a Nikon 90i widefield microscope using Nikon's NIS-Elements v. 4.30 software. A Nikon D-DP polarizer was inserted into the microscope and the light polarized to image birefringence within the samples. The images were acquired using the lambda and large area functionality of the ND Acquisition dialog box.

Results: We were able to identify polarizable material in digital images using the automated method described above. Certain polarized material was more difficult to characterize. Example images (suture granuloma) demonstrate an automatically acquired brightfield image (A), a polarized image (B), and a merged image (C).

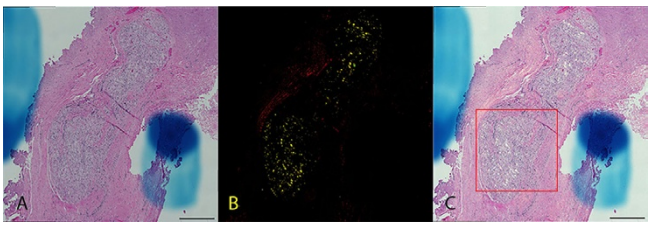

Conclusions: The demonstration of polarized elements present within tissue is critical for certain diagnostic entities. Incorporating polarizable functionality within digital whole slide images is important if whole slide imaging is to be adopted for general pathology signout. We found variability in the ability of this method to identify all types of polarizable material. We recommend that future versions of whole slide imaging devices incorporate polarizers into the product design in order to fill this void.

1561 Stain Normalization in Digital Pathology Images Using Deep Learning

Andrew Janowczyk, Ajay Basavanhally, Anant Madabhushi. Case Western Reserve University, Cleveland, OH; Inspirata, Tampa, FL.

Background: Variances in the visual appearance of digital histopathology slides may be attributed to specimen preparation (e.g., staining protocol) and scanner platform. While digitization of pathology slides makes them amenable to quantitative image analysis methods, many of these tasks, such as nuclei segmentation, tend to be highly sensitive to scanner and stain specific image variations. In this work we present a new color standardization approach to address these variations. The rationale behind our approach is that similar tissue types (e.g. stroma, nuclei), independent of their chromatic differences, tend to be clustered in the feature space. We use a deep learning approach that uses multi-layer neural networks to successfully identify tissue partitions in an automated way. Once the partitions are identified, histogram equalization to a reference template can be done on a per partition basis.

Design: We evaluate our approach using 2 specially prepared datasets to mirror real-world factors: (a) 5 breast biopsy slides scanned 3 times on a Ventana scanner and once on a Leica scanner to measure inter/intra scanner variances, and (b) 7 adjacent slices from a gastro-intestinal biopsy scanned after using 7 different staining protocols (HE, HoE, HuE, oHE, oHoE, uHE, and uHuE, where "u" and "o" indicate over- and under-staining of the specified dye) to measure stain variances. In both, reduction in variance of intensity distributions was evaluated by computing the sum of squared differences (SSD) between each of the RGB channels.

Results: We are able to reduce the SSD of inter scanner variability (.047) to within intra scanner variability (.0473) as well as reduce intra scanner SSD (.01). We were also able to bring drastic stain protocol differences (see Figure) into intra scanner range (.05). In both experiments we compared our approach to the state-of-the-art and show either comparable or superior results in terms of reduced SSD.

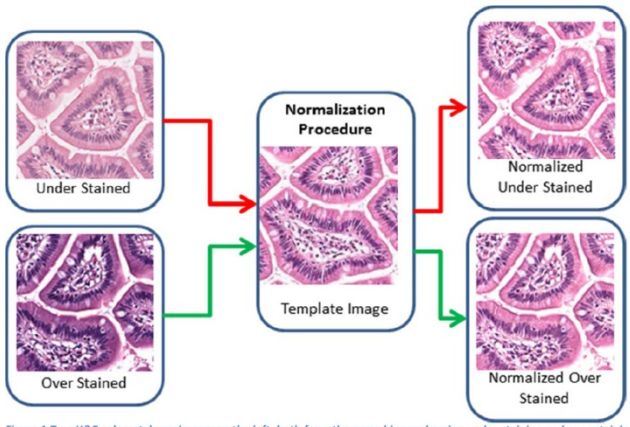

Figure 1 Two H&E colorectal specimens, on the left, both from the same biopsy showing under-staining and over-staining of H&E, demonstrating the severity of chromatic differences which tend to inhibit consistent performance from automated image analysis algorithms. After selecting a desired template image (middle), our approach is successfully able to normalize both images to the template image (right).

Conclusions: Normalization of digital histopathology images is critical to improve the robustness of quantitative image analysis approaches. Our approach has shown the capacity to reduce (a) variability in H&E images to within intra-scanner variance and (b) stain protocol variances down to intra scanner levels.

1562 Fully Automated, Accurate, and Efficient Segmentation of Cancer Nuclei in Breast Pathology Images

Andrew Janowczyk, Hannah Gilmore, Anant Madabhushi. Case Western Reserve University, Cleveland, OH; University Hospitals, Cleveland, OH.

Background: The morphology and structural organization of nuclei are not only a critical component in breast cancer grading schemes but have been correlated with disease prognosis and outcome. Digitization of pathology slides has enabled the application of computerized image analysis methods on these tissue images and a number of these methods have focused on automated nuclei detection. In this work we present a resolution adaptive deep learning (RADL) solution (a paradigm employing large artificial neural networks) which utilizes a hierarchical approach to reduce computation time for pixel-wise analysis of large images. In our RADL approach, at each level of the hierarchy a deep learning (DL) network is trained to determine if a subsequently higher level of magnification is needed to correctly delineate the nuclei. As a result, images at the target resolution contain many fewer pixels to analyze, resulting in large efficiency gains.

Design: Our approach was evaluated on digitized slides obtained from 141 estrogen receptor positive breast cancer patients. Each slide corresponded to a whole slide biopsy stained with H&E which was then subsequently scanned at 40x magnification. From these large images we cropped 1,000 x 1,000 regions of interest to evaluate our nuclei segmentation approach. An expert annotated over 12,000 nuclei across the 141 images.

Results: We compared RADL with a DL approach that was only employed at a single magnification and found computational efficiency savings of over 85%. At the same time, the nuclei detection accuracy was found to be comparable (see Figure) across RADL and DL (97% vs 99%). Additionally the true positive rate across RADL and DL was comparable (.835 vs .850). These performance indices also compare favorably with other state of the art nuclear segmentation approaches for digital pathology images.

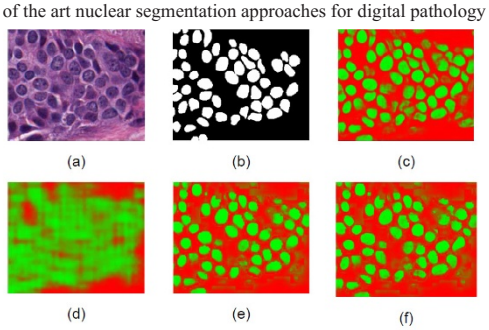

Figure 1 Comparison of (f) RADL versus (c) applying DL solely to the highest magnification. The original image is shown in (a) with its ground truth in (b). When applying the network directly to the top layer which is at a magnification of 40x, probability map (c) is obtained, where the more green a pixel is, the more likely it is to belong to the nuclei class. When looking at (d), the lowest level (4x), the probability map already appears to clearly indicate where the nuclei are. Unnecessary computations are thus avoided on all of the red pixels. Mapping the results of RADL up to (e) 10x magnification already reveals much more accurate results. When the results of RADL are mapped up to (f) 40x magnification, the results in (f) are nearly identical to that obtained in (c), but faster by 6x.

Conclusions: We presented a resolution adaptive deep learning (RADL) scheme for nuclear segmentation in histology images. Our RADL approach enables identification of candidate nuclear locations at a lower magnification than required via a traditional deep learning scheme at higher resolutions, resulting in accurate and highly efficient segmentations of nuclei.

1563 Validation of the Mobile Whole Slide Imaging as a Low Resource Acquisition and Transport Technique for Microscopic Pathological Specimens

Fatima-Zahra Jelloul, Louis J Auguste, Dhaval H Palsana, Tawfiqul Bhuiya, Michael J Esposito. Hofstra North Shore-LIJ, Bellerose, NY; New York University, New York, NY.

Background: Mobile Whole Slide Imaging (mWSI) was developed to help reduce telepathology cost in developing countries. It is an affordable system consisting of a standard light microscope, a mobile smart phone for imaging the slide through the microscope (iPhone 5s in this study) and a 3D printed adaptor configured to receive and position the phone's camera on the eyepiece of the microscope. The aim of this study was to validate mWSI use by comparing histopathological diagnoses using mWSI to light microscopy diagnoses from the original matched glass slides.

Design: 59 routine cases from biopsies and resections diagnosed at our institution during August 2014 were studied. One slide best representing the original diagnosis was chosen. mWSI were obtained by scanning the original glass slides from all cases at 20X magnification. The scan consisted of acquiring multiple panoramic images for multiple adjacent rows across the slide. Once the entire slide was captured, the images were transferred onto a computer and fed into an image stitching algorithm and a single composite image or mWSI was created. 2 pathologists blinded to the original results, diagnosed mWSI and the glass slides after a washout period of 4 months. mWSI and glass slides diagnoses were compared and concordance rates were calculated for each reviewer.

Results: The 59 scanned cases included 31 benign and 28 malignant cases. The concordance rate between mWSI and glass slide diagnoses was 95% (56/59) for both reviewers. 2 discordant cases with major clinical implication were misdiagnosed by both reviewers; one from a breast biopsy with DCIS and focal microinvasion. The microinvasion was missed on mWSI but confirmed after review of mWSI. The second case was from a thyroid resection where follicular variant of papillary carcinoma was misdiagnosed as follicular adenoma on mWSI. This case was also reviewed; the discordance was due to sub-optimal image with pixelation on high power, precluding assessment of nuclear details. The third discordant case for reviewer 1 was serous carcinoma of uterus misdiagnosed as endometrioid carcinoma on mWSI. For reviewer 2, the third discordant case was leiomyoma misdiagnosed as fibroma-thecoma on mWSI.

Conclusions: This study indicates that mWSI offers excellent diagnostic accuracy. This affordable system can be used as an adequate telepathology tool to help expedite the diagnostic process in low-resource environments and provide patients with better health outcomes.

1564 The Importance of Quality Control in Report Translation in an International Telepathology Practice

Christopher J Kim, Guofeng Wang, Li-Rong Chen, Jianyu Rao. University of California, Los Angeles, Los Angeles, CA; Zhejiang University School of Medicine, Hangzhou, China.

Background: Whole-slide imaging (WSI) technology has the potential to provide global access to internet-based subspecialist pathology consultative services. We discuss the experience of first adopters of international telepathology at Second Affiliated Hospital of Zhejiang University (SHAZU) and investigate pathology report translation services and their impact on patient care, particularly with regard to the translation of English pathology reports to Chinese in a clinical telepathology setting.

Design: We reviewed records from the last 3 years (January 2013 to July 2015) of a telepathology program between pathologists at SHAZU and University of California, Los Angeles. Consultations originate as WSI using an internet-based platform. Consult reports are electronically delivered to the originating pathologist for language translation from English to Chinese. All cases undergo secondary review from a pathologist fluent in both languages before finalization at SHAZU. Biannually, 10% of reports are randomly selected for quality control (QC). Reports with discrepancies between the original and translated report were further graded as Major or Minor errors depending on the presence or absence of potential clinical or prognostic implications, respectively.

Results: Of 988 total cases, 114 (11.5%) were investigated in the language QC program. Of these, 12 (10.5%) had Minor errors and 2 (1.8%) had Major errors. Minor errors were related to omission of portions of the original report (9/12) or minor typographical errors (3/12) of no significance. Major errors had no clinical impact and were related to imprecise translation of medical nomenclature in one case ("hemorrhage" mistranslated as "hemangioma") and mistranslation of organ site ("endocervical " mistranslated as "endometrial") in the diagnostic comments of a radical hysterectomy with tumor of ambiguous origin.

Conclusions: Although no significant errors with clinical impact were detected through quality control programs, our findings suggest that language translation errors have the potential to be a root cause of serious medical error. Our preliminary experience reinforces the importance of systematic quality assurance measures and highlights the critical role of experienced bilingual pathologists and support staff. With the growth of international telepathology, we feel there will be a critical need for more detailed studies on the quality and clinical impact of language translation in pathology consultative reports.

1565 MRI Derived Histologically Trained Maps of Epithelium Density Predict Prostate Cancer Presence

Peter S LaViolette, Amy Kaczmarowski, Kenneth A Iczkowski, Kenneth Jacobsohn, Paul M Knechtges, Mark Hohenwalter, William See. Medical College of Wisconsin, Milwaukee, WI.

Background: Radiological-pathological (Rad-Path) correlation has recently allowed the validation of prostate cancer imaging technology. The next generation of imaging biomarkers will be created using the combination of these two modalities for training machine learning algorithms to predict cancer presence with non-invasive imaging.

Design: Ten prostatectomy patients were imaged ≤2 weeks pre-op using a 3T MRI machine (GE) and quantitative diffusion weighted imaging. Custom-designed, 3D-printed slicing molds were used to cut tissue to match the orientation and 4mm MRI slice thickness. Whole-mount sections were digitally segmented using custom code developed in Matlab. Segmentation features included lumen, stroma, and epithelium/nuclei. Digitized histology was co-registered to T2-weighted MRI using Matlab software and non-linear warping. A partial least squares regression (PLS) machine-learning algorithm was trained with co-localized MRI voxel values and corresponding histology features. A leave one out approach was used to generate predictive maps of histological features for each patient using the histology and corresponding MRI values from the other 9 patients. Maps of each feature were then compared to Gleason (G) graded whole mount histology.

Results: All 10 patients had benign/atrophic glands (B) and G3 cancer. Seven patients had G4 and one patient had G5. Quantitative MRI derived PLS trained maps of epithelium/nuclei were most predictive of the location of cancer. In all 7 cases with focal G4+ cancer, the predictive maps indicated abnormally high epithelium percentages co-localized with pathologically confirmed G4+ cancer. In nine of ten cases with regions of G3, hotspots of epithelium/nuclei percentages co-localized with the pathologically confirmed regions.

Conclusions: We generated machine-learning trained maps of histological features based on non-invasive MR imaging. We found that locations with high epithelium/nuclei indicated regions of G3+ cancer. More research is necessary to determine how this new machine-learning based biomarker should be used for diagnostic purposes.

1566 Evaluating Reproducibility of Computer Extracted Histologic Image Features for Predicting Biochemical Recurrence in Prostate Cancer: A Multi-Site, Multi-Scanner Study

Patrick Leo, George Lee, Anant Madabhushi. Case Western Reserve University, Cleveland, OH.

Background: Computer extracted image features describing gland appearance and texture from routine H&E slides of surgical specimens have been suggested to be associated with outcome prediction of prostate cancer (CaP). Variations between stain batches and the whole-slide scanner used to digitize specimens can affect the final appearance of the images and hence adversely affect feature values associated with biochemical recurrence (BCR) following radical prostatectomy (RP).

Design: Our goal was to quantify the stability of 242 computer extracted histologic image features (51 global and 26 local graphical arrangement of glands, 100 gland shape, 39 gland orientation disorder, and 26 intensity texture features) extracted from 80 H&E stained RP specimens (see Fig. 1) with Gleason sum 7 and no BCR within 5 years of surgery across 4 different sites. A feature was identified as stable between two cohorts if that feature's values were not different between the cohorts at the $p<.05$ level by Wilcoxon rank sum test. An intra-dataset comparison of features across 1000 random splits of each dataset tested the null hypothesis that features are stable within a single dataset.

Results: As shown in Fig. 1(m) the average feature was different in less than 5% of intra-dataset comparisons. This appears to suggest that instability between datasets may not be due to chance. Fig. 1(n) shows inter-dataset instability in 20-56% of comparisons. Gland shape and disorder features were most and least stable respectively being different at rates 4 and 14 times greater than expected from chance. This instability appears to reflect variability in gland segmentation due to tissue staining and scanning variance.

Conclusions: We found significant differences in feature values between datasets from different institutions. Shape features were most stable and disorder features least stable. These findings highlight the need for identifying 1) features which are robust to staining variability, 2) techniques which can standardize digital images, and 3) a more consistent protocol for preparing H&E slides. Addressing one or more of these will be key to developing robust and predictive decision support tools for use by pathologists.

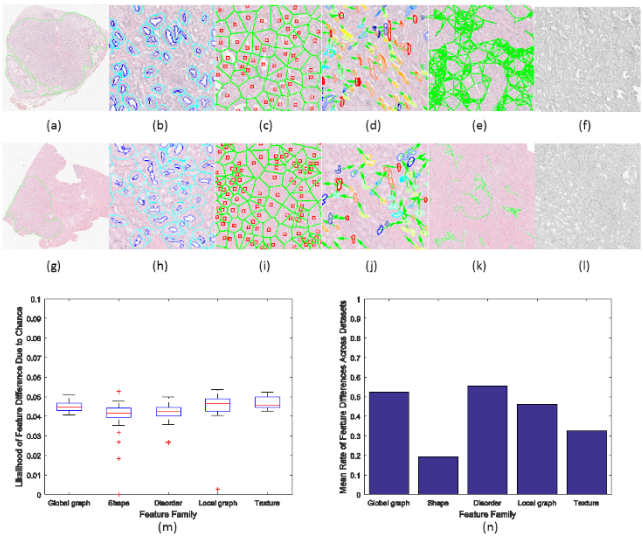

Figure 1: Feature extraction process for a patient from Laboratory 1 (a-f) and Laboratory 4 (g-l). (a)(g): Cancerous regions annotated by expert pathologist. Automatically extracted features corresponding to (b)(h): Gland shape, (c)(i): Global gland graphs, (d)(j): Gland disorder, (e)(k): Local gland graphs, and (f)(l): Haralick intensity texture. (m): Intra-dataset instability rates grouped by feature family when comparing features extracted from random splits of images within the same site. (n): Mean instability rate of each feature family when comparing features extracted from images from different sites.

1567 The Use of Computer Vision in the Differential Diagnosis of Ovarian Carcinomas

Xinyan Li, Vassilios Morellas, Nikolaos Papanikolopoulos, Alexander M Truskinovsky. University of Minnesota, Minneapolis, MN; Roswell Park Cancer Institute, Buffalo, NY.

Background: We recently showed that computer vision can successfully distinguish carcinomas of the uterus, prostate and breast from these organs' benign tissues, and leiomyosarcomas from leiomyomas and leiomyoma variants. Differential diagnosis between the types of ovarian carcinoma can be difficult for pathologists based on histomorphology alone and often requires immunostains. Here we investigate whether computer vision can differentiate between the four major types of ovarian carcinoma.

Design: We scanned on a digital slide scanner at x50 magnification 6 H&E-stained slides each of high-grade serous, endometrioid and clear cell carcinomas of the ovary and 3 slides of mucinous carcinomas. The color images were manually annotated to train the classification algorithm, then sliced and broken down into overlapping blocks of 200 x 200 pixels. In all, we were able to obtain 4970 useful blocks for serous, 3764 for endometrioid, 1460 for mucinous and 4869 for clear cell carcinoma. We then randomly selected roughly the same number of samples from each tumor class to construct our database. We used Region Covariance Descriptor (RCD) to extract abstract features from the raw image and applied K-nearest neighbor (KNN) search to recognize different tumor types. We selected texture features, i.e. I (intensity of the image), Ix, Iy (gradient of the image along x and y axis) and $\sqrt{(I_x^2+I_y^2)}$ (its magnitude) to construct the RCD. Our previous studies showed that selecting this set of features can expedite the analysis, while maintaining the analysis quality. After RCDs were generated, samples from different tumor pools were evenly yet randomly chosen to build our database. 10-fold cross-validation was then implemented to evaluate the overall performance of the computer assistant tool on this database.

Results: Starting from a database size of 4500, we could achieve an accuracy of 81% of differentiation among all 4 types of carcinoma, increasing to 84% with the database size of 9000. The accuracy of differential diagnosis was 90% between serous and endometrioid carcinomas, 93% between endometrioid and mucinous carcinomas and 94% between serous and clear cell carcinomas. On a 3-dimensional KNN graph, clear cell carcinomas stood out the most from the other carcinoma types.

Conclusions: This study shows that computer vision can not only distinguish between benign and malignant tissues but, notably, differentiates with great success between the types of malignant tumors of the same organ, a non-trivial task even for human pathologists.

1568 Analysis of Available Clinical Trials for Targeted Therapies in Solid Tumors

Susan Mockus, Sara E Patterson, Rangjiao Liu, Cara Statz. The Jackson Laboratory for Genomic Medicine, Farmington, CT.

Background: The use of next-generation sequencing (NGS) assays for somatic tumor profiling has gained significant momentum over the past few years. The goal of these NGS assays is to connect a patient's somatic mutation to a targeted therapy. There are a limited number of FDA-approved therapies for specific mutations. Therefore, the clinician may use an FDA-approved therapy as an off-label or enroll the patient in a relevant clinical trial. Location, availability, and eligibility of clinical trials can be rate limiting.

Design: A Clinical Knowledgebase (CKB) was designed and manually curated over the last two years to support patient reporting for a 358-gene panel. US and Canada clinical trials were automatically retrieved from clinicaltrials.gov through a cron job and then manually curated for data elements that cannot be programmatically retrieved from the registry. 2,453 open clinical trials were analyzed in CKB for distribution of clinical trials by targeted therapy, drug class, and mutation.

Results: Bevacizumab and everolimus were found in the greatest number of open interventional clinical trials with 176 and 99 open trials, respectively. In trials using bevacizumab, glioblastoma was the most common tumor type and in trials using everolimus, ERBB2 (HER2)-negative breast cancer was most common. Solid tumor types with the highest number of open trials were NSCLC, melanoma, ERBB2 (HER2)-negative breast cancer, prostate cancer, and glioblastoma. 105 indications were found in only a single clinical trial. Clinical trials with eligibility requirements for mutations in BRAF, KRAS, EGFR, PIK3CA were highest, while less characterized mutations in AKT2, DDR2, VEGFB, and RAD51C were among those included as eligibility criteria in the fewest clinical trials. VEGFR inhibitors had the highest number of trials, followed by KIT, PDGFR, RET, CSF1R and mTOR inhibitors. Vemurafenib in melanoma had the highest number of trials that were withdrawn or terminated.

Conclusions: Analysis of available clinical trials for an NGS assay in oncology can provide a landscape for the overall actionability of a gene panel and enable better design of gene panels. Further, this analysis can expose weaknesses in availability of targeted therapeutic intervention, by enabling visibility into a lack of trials recruiting on specific mutations, drug classes, and/or indications. This may serve to direct research to these areas, ultimately increasing opportunities for treatment and improving patient care.

1569 Hierarchical Clustering of Mutational Profile of Uterine Carcinosarcomas and Comparison with Uterine Endometrioid and Serous Adenocarcinomas

Amir Momeni Boroujeni, Elham Yousefi, Remegio Maglantay, Raavi Gupta, Ning Neil Chen. SUNY Downstate Medical Center, Brooklyn, NY.

Background: Understanding the genetic profile of cancers is integral in evaluation of their pathophysiology and paves the way for targeted therapy in patients. Uterine carcinosarcomas (UCS) are invariably high-grade tumors with poor prognosis. These tumors are biphasic with sarcomatous and carcinomatous elements and are now believed to originate as a carcinoma that undergoes sarcomatous transformation. In this study we aim to compare the mutation profile of uterine carcinosarcomas with uterine endometrioid (UEA) and uterine serous adenocarcinomas (USA) using cluster analysis.

Design: Mutation data for 57 UCS cases along with 375 UEA and 112 USA cases were extracted from the TCGA database. A mutation network matrix was calculated for each group of cases and imported into the Netminer software. Hierarchical cluster analysis was performed along with power centrality calculation for each of the mutated genes in the pool. The networks were then compared along the three groups.

Results: TP53, FRG1B, FBXW7, PIK3CA, PPP2R1A, MUC4, PTEN, CHD4 (4.45, 2.97, 2.61, 2.38, 2.31, 2.26, 2.19 and 2.16 respectively) have the highest centrality power and form the core of the mutation clusters within UCS (figure 1). Hierarchical cluster analysis identifies 8 main subclusters in UCS mutation network which account for 100% of cases. These clusters correspond with mutation clusters in 50.66% and 39.28% of UEA and USA cases respectively (Figure 2).

Conclusions: Previously it has been suggested that UCS start as UEA or USA and transform into UCS after acquiring additional mutations. Our analysis show that UCS share gene mutation subclusters with both UEA and USA. Combining these subclusters account for all of the mutations in UCS further supporting the hypothesis that UCS originate as either UEA or USA with mutation in genes such as FRG1b and MUC4 playing a unique but still unknown role in progression of UCS.

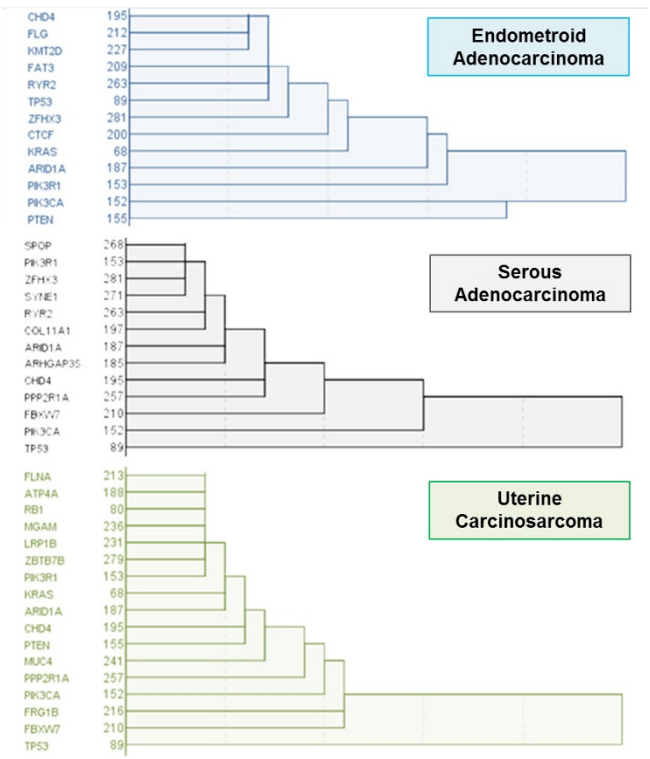

Mutation Clusters	USA†	UEA†	UCS†
Cluster 1: FLNA + ATP4A + RB1 + MGAM + LRP1B + ZBTB7B + PIK3R1	4.46%	28.53%	47.36%
Cluster 2: Cluster 1 + KRAS + ARID1A	8.92%	39.46%	64.91%
Cluster 3: Cluster 2 + CHD4 + PTEN	15.17%	48.26%	70.17%
Cluster 4: Cluster 3 + MUC4	15.17%	48.26%	77.19%
Cluster 5: Cluster 4 + PPP2R1A	22.32%	48.53%	82.45%
Cluster 6: Cluster 5 + PIK3CA	28.57%	50.40%	87.71%
Cluster 7: Cluster 6 + FRG1B + FBXW7	33.92%	50.40%	91.22%
Cluster 8: Cluster 7 + TP53	39.28%	50.66%	100%

† USA: Uterine Serous Adenocarcinoma, UEA: Uterine Endometroid Adenocarcinoma, UCS: Uterine Carcinosarcoma

1570 The Influence of Prior Laboratory Values and Patient Demographics on Physician Test Ordering: Capturing Non-Linear Effects within a Population-Based Retrospective Cohort Study

Eric Morgen, Christopher Naugler. Mount Sinai Hospital, Toronto, ON, Canada; University of Toronto, Toronto, ON, Canada; Calgary Laboratory Services, Calgary, AB, Canada; University of Calgary, Calgary, AB, Canada.

Background: The ordering of repeated laboratory tests is an important source of unnecessary laboratory testing, and can be influenced by patient factors, medical findings, and physician factors. These influences are not well described, and quantifying them is essential to understanding why tests are ordered, which may be potentially redundant, and how to direct medical policy. At the same time, a repeat test may represent a universal outcome indicating (in many scenarios) clinical concern about the results of the initial test, and provides a window onto physician perceptions of laboratory test values.

Design: We conducted a retrospective cohort study of 24 common laboratory tests using a regional population sample of 100,000 patients identified from a laboratory informatics database. Patients were selected with one or more index tests in 2010 and uniform follow-up of 1 year. The influence of demographic factors (age and sex), testing location, and index test results on repeat orders was investigated using Cox proportional hazards modeling and extended via restricted cubic splines to capture non-linear relationships using R (v. 3.2.0) and the RMS package.

Results: Patients older than 65 were more likely to be retested (HR=1.52, $p<0.001$), while patient gender exerted only a minor influence. Patients tested in an emergency department, hospital clinical, or inpatient ward were more likely to be retested (HRs 2.2, 2.7, and 6.1; p-values <0.001), relative to community clinics. Modeled non-linear hazard ratio for retesting increased for test values as they approached and exceeded abnormal limits for a test (including a substantial increase within normal limits). For particular tests, the hazard of retesting also increased in the direction where no abnormal limit was defined.

Conclusions: Patient age and test result values were important factors influencing the likelihood of repeated testing, and often showed strongly non-linear relationships. Certain associations, such as increased retesting before abnormal limits are reached, or in directions with no abnormal limit, may hold promise as targets for reduction of unnecessary tests. Finally, non-linear modeling of the relationship of test values to repeated testing appears to provide a data-derived illustration of perceptions of clinical relevance by ordering physicians.

1571 A Bioinformatics Software Pipeline for Identifying Causal Genetic Mechanisms of Antibiotic Resistance in Bacterial Pathogens

Karthikeyan Murugesan, Xinran Li, Pramod Mayigowda, Henry Lin, Guiqing Wang, Abhay Dhand, Weihua Huang, John T Fallon, Nevenka Dimitrova. Philips Research North America, Cambridge, MA; New York Medical College, Valhalla, NY.

Background: The ESKAPE pathogens are known to be major culprits of Hospital Acquired Infections reported in the US and the biggest cause of concern is their growing antibiotic resistance. Annually, mortality due antibiotic resistance alone is over 700,000 worldwide with 23,000 of those in the US.

Design: Whole genome sequencing of these pathogens combined with their clinical profiles for antibiotic phenotypes are a great repertoire of knowledge for bioinformatics to provide meaningful insights into the genomics, evolution, and diagnosis of antibiotic resistance. Real time antibiotic profiles of patients could drive clinical decisions on antibiotic choice, dosage, and stewardship.

We try to address this problem by using bioinformatics algorithms to integrate genomic data with antibiotic resistance profiles to characterize and identify mutations, genes, and mobile genetic elements associated with resistance. Our algorithmic pipeline consists of three modules – genes associated with resistance (GAR), SNPs associated with resistance (SAR), and the Antibiotic Resistance (AbRes) module. The GAR module identifies genes associated with resistance while the SAR module calls variants on the sequences and finds variants enriched amongst the resistant pathogens. The AbRes module consolidates information from the previous two modules to provide specifics on non-synonymous mutations in genes which could constitute a resistance cassette associated with antibiotic resistance.

Results: We have tested our pipeline to understand the mechanisms of daptomycin resistance in nosocomial infections of Enterococcus faecium . We sequenced 149 E. faecium isolates of MLST type ST736 from 106 patients over 55 months at the Westchester Meical Centre, New York. The modules were tested on a set of E. faecium sequences selected for quality based on parameters like read depth, coverage, variant calls and genes covered.

Preliminary analysis revealed impactful genes and non-synonymous mutations associated with functionally well-known two component regulatory systems, transcriptional regulators, transposases, sortases, DNA binding and relevant cell wall proteins.

Conclusions: Interestingly, some of these genes and mutations were a part of a larger operon network which could be putative resistance cassettes.We plan to evaluate these results experimentally with our academic and clinical collaborators to assess their biological and clinical significance.

1572 Turn Around Time Monitoring in Anatomical Pathology: Time to Event Analysis

Nickolas Myles, Douglas Filipenko, Marin J Trotter. University of British Columbia, Vancouver, BC, Canada; Providence Healthcare, Vancouver, BC, Canada.

Background: Turn-around time (TAT) monitoring in anatomical pathology is a key performance indicator, but TAT methodology is rarely a focus in the pathology literature. TAT is an example of non-normally distributed (right skewed) variable, requiring transformation or use of a semi-parametric approach. In addition, the mean TAT does not give the proportion of cases signed-out at different clinically sensible time points, nor does it provide trend information. The aim of this study is to apply survival analysis (time to event analysis) to TAT monitoring, using breast core biopsy TAT as an example.

Design: We extracted TAT data (2010-2014) for all breast core biopsies processed in our department (n=4,118), time of accessioning and time of sign-out for each case. There were no sensored cases. We then built a histogram and ran Kaplan-Meier analysis, using 1-minus-survival (time to task completion) plot, and stratified the data by the calendar year. Log-rank test was used to compare the differences in TAT between calendar years.

Results: The model fit proportional hazard assumption. We visualised the TAT by histogram, displaying right-skewed distribution.

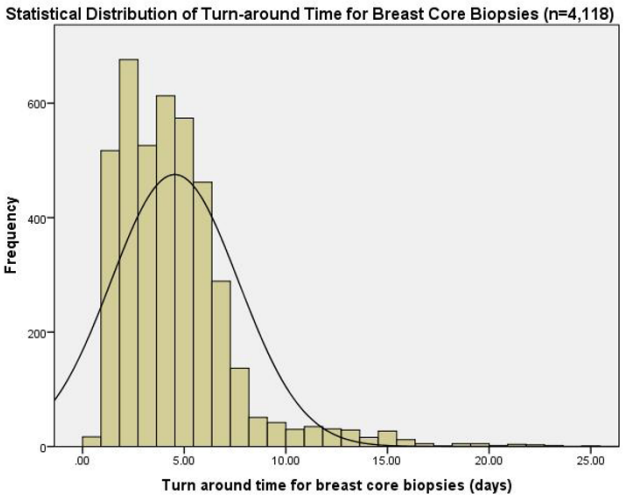

The Kaplam-Meier curves show notable similarity over the years, with a small yet statistically significant difference in TAT over the years (log rank test, $p<0.0001$, from median 4.3 (95%CI 4.1-4.6) days in 2010 to 3.8 (95%CI 3.4-4.2) days in 2014).

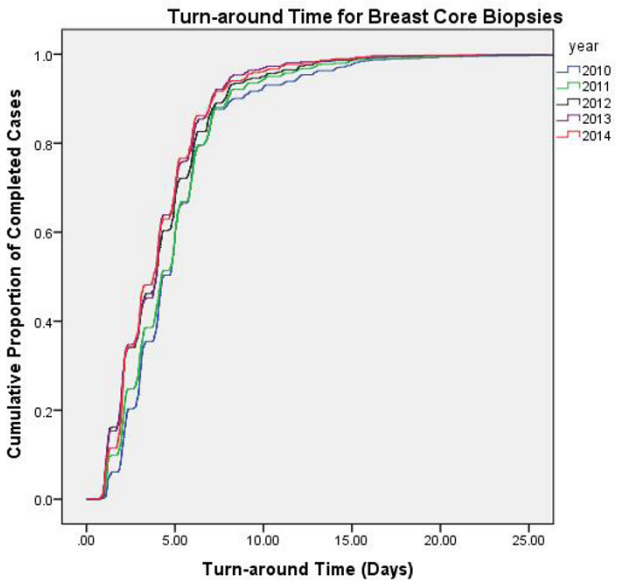

Conclusions: Kaplan-Merier (aka time to event) analysis is informative method of monitoring TAT in anatomical pathology. It displays trends and internal dynamics in the laboratory over time and is more informative than point estimates of mean and median TAT. Furthermore, although not shown in the abstract, it is applicable to monitoring of individual pathologist turn-around time and allows for multivariate adjustment to case complexity, daily workload, and use of ancillary methods.

1573 Development of New Fluorescence Virtual Slide System Equipped with the Liquid Crystal Filter Unit

Hiroyuki Nozaka, Tomisato Miura, Zhongxi Zheng. Hirosaki University, Hirosaki, Aomori, Japan.

Background: Fluorescence observation is one of useful high sensitivity method for protein or gene expression analysis in histopathology. However, fluorescence attenuates in a short time, fluorescence virtual slide is necessary for the long-term storage of slide. Meanwhile, fluorescence observation requires the optical band-pass filter corresponding to each fluorescent dyes. It is difficult for multi-color analysis to mount a large number of filters in the limited space inside the virtual slide system. Therefore, it is required that the variable wavelength band-pass filter unit for multi-color analysis. The aim of this study is development of new fluorescence virtual slide system.

Design: 1) System configuration

We developed the variable wavelength band-pass filter which is made of the liquid crystal. The filter unit is consists of Polarizer, Phase difference plate, glass plate, liquid crystal and hardener. We developed new liquid crystal material made of T type chiral compound to get high speed response and high contrast. This filter unit is possible to set specific wavelength by voltage, and it was mounted on original specification virtual slide system.

2) System evaluation

For comparison of performance both conventional optical filter and liquid crystal filter, we evaluated light transmittance rate, S/N ratio, and quality of the virtual slide image. Tumors were collected from 20 patients diagnosed with primary breast cancer. FISH and IHC by SAB method with fluorescence-labeled antibody was performed for HER2 on FFPE tissue sections.

Results: The liquid crystal filter was selectively passed through fluorescence. Light transmittance rate of the liquid crystal filter unit was showed between 15% and 30%. S/N ratio was showed high (20~30db). The image quality was good for diagnosis both filter units.

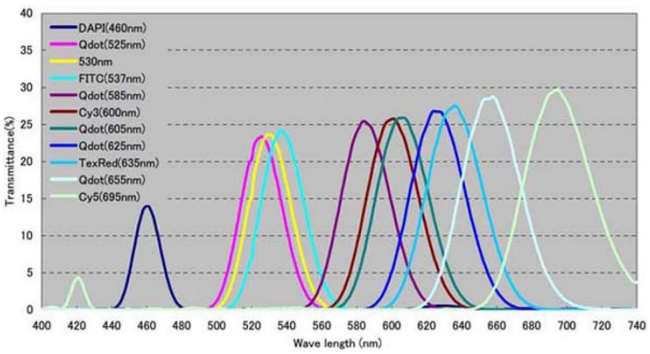

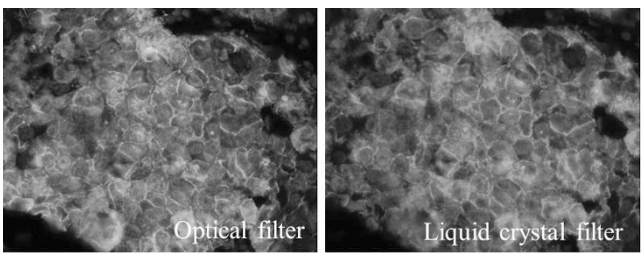

Conclusions: The fluorescence virtual slide system equipped with the liquid crystal filter unit is useful for multi-color fluorescence imaging.

1574 Pathology-Driven Cloud-Based Mutidisciplinary Team Meeting Software

Fionnuala O'Connell, Tim Manning, Brian Kelly, Noel Murphy, Paul Walsh, Tara Jane Browne, Michael W Bennett. Cork University Hospital, Cork, Ireland; nSILICO, Cork, Ireland; Health Innovation Hub, Cork, Ireland.

Background: Cancer care is moving from specialty-based to patient-centered approach, where all aspects of care are considered in multidisciplinary team (MDT) meetings. MDT meetings are logistically demanding requiring correlation of clinical, radiology and pathology data. Due to case volume the meeting has to be highly efficient. Electronic health record (EHR) collation of the data into a single rapidly accessible source may not be possible in the time available. With paper records much time is spent trying to ascertain the precise clinical situation. The efficiency of the MDT meeting is difficult to estimate and no meaningful data can be retrieved from the EHR/paper records thus an important opportunity for data analysis is lost. Reliance on a paper based system also has an associated risk of error.

Design: LEAN process analysis was used to determine deficiencies in the MDT process at a large cancer center. To address these limitations we developed a cloud-based software application to assist in coordination and execution of MDT meetings via a comprehensive data capture and management system for electronic medical records. The system was developed using an agile software development methodology, with frequent piloting with users in trial scenarios, to satisfy needs of clinical, administrative and patient stakeholders. Precise, efficient data entry was developed through usability analysis. Custom visualisations and data analytics were implemented to provide process feedback and trend analysis. Rigorous attention was paid to patient safety, security and privacy, by conforming to HIPAA rules, through the use of physical, technical and administrative safeguards. These safeguards include our custom implementation of access control, automatic log-out, encryption/decryption, audit controls, authentication, integrity controls and transmission security.

Results: The system facilitates ease of access, data entry and provides visualisation of concordant/discordant cases with comprehensive data analytics, which provide planning/management intelligence. It is available 24/7 to users via a cloud based platform that is secure to HIPAA standards and includes a traceable audit trail.

We present a high-level overview of system architecture, user interface, security framework, and reporting and analytics output. We demonstrate that operation of the tool in an MDT setting allows members to rapidly record decision-making across all key dimensions.

Conclusions: MDT software optimises MDT meetings and provides a basis for managing cancer care through the use of cloud based data analytics.

1575 Exploring Oculus Rift for Viewing Whole Slide Images in a Virtual Reality Environment

Liron Pantanowitz, Navid Farahani, Brian J Kolowitz, Robert Post, Teppituk Krinchai, Isthiaque Ahmed, Sara E Monaco, Jeffrey L Fine, Jon Duboy, Douglas J Hartman. University of Pittsburgh Medical Center, Pittsburgh, PA.

Background: Whole slide images (WSI) in pathology are typically viewed in two dimensions on a monitor. To the best of our knowledge, we are not aware of WSI being viewed in a virtual reality (VR) environment. VR artificially allows users to be immersed in and interact with a computer-simulated world. Oculus Rift (OR) is a head-mounted display that creates such a VR environment, usually for gaming. Our aim was to explore the use of OR for examining digital pathology slides.

Design: An Oculus Development Kit 2 (DK2) was connected to a 64-bit computer (HP Z440 Workstation, Intel Xeon E5-16650v3, 32GB DDR4-2133, NVIDIA GeForce GTX Titan X GPU, 512GB PCIe SSD, 1TB 7200RPM HDD) running Microsoft Windows 7 and Virtual Desktop. Glass slides from 10 lymph nodes (5 benign, 5 malignant) were scanned (Aperio XT scanner, Leica). Three pathologists were asked to review these WSI on a 24-inch LCD monitor (HP ZR24w) and with OR (see figure). Their diagnoses and time to read slides were recorded. They also rated image quality (1-10), ease of navigation (1-10), and diagnostic confidence (1-10) for both modalities.

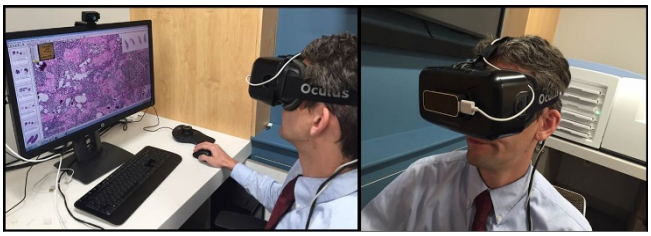

Results: WSI were able to be viewed in a VR environment using the OR. There was 100% diagnostic concordance with both modalities. Time to read WSI on the LCD monitor averaged 80 seconds (range 45 sec – 3.5 min) and using Oculus 74 seconds (range 20 sec – 2min 40 sec). Pathologists similarly rated image quality, ease of navigation, and diagnostic confidence for both sessions.

Conclusions: Using Oculus Rift to view and navigate pathology WSI in a virtual environment is feasible. However, image quality is limited by the device's resolution (1920 x 1080). Although the VR atmosphere provided pathologists with a wide field of view that simulates microscopy, reading slides with this novel display did not enhance their navigation of digital slides. The Leap Motion Controller is being tested to use hand gestures instead of input devices such as a keyboard or mouse, which may improve the use of OR for reading WSI.

1576 Validation of Whole Frozen Section Slide Image Diagnosis in Surgical Pathology

Vamsi Parimi, Adrianna Borys, Yi Zhou, Roberto Gamez, Ewa Borys, Maria M Picken, Dariusz Borys. Loyola University Medical Center, Maywood, IL; NYU, New York, NY.

Background: Automated whole slide imaging (WSI) using high-resolution scanners is becoming increasingly popular platform in
surgical pathology clinical practice for formalin fixed paraffin embedded stained sections but not so for frozen section (FS) diagnostic evaluation. We report results of inter and intraobserver variability in the evaluation of WSI-FS digitized adenocarcinoma slides among reviewers to that of original glass slide (G-FS) interpretation.

Design: A total of 110 FS adenocarcinoma cases (172 specimens and 395 glass microscope slides) from random sites from 2013 and 2014 are scanned by Aperio CS2 slide scanner (Leica Biosystems, San Diego,CA, USA). These cases were originally interpreted on glass slides by multiple pathologists. In our study, 5 surgical pathologists independently evaluated WSI-FS slides (including deep cuts) necessary to make a final diagnosis on eSlide Manager (Leica Biosystems) platform. Diagnostic discrepancies

are studied at specimen and case level and a consensus was reached. No clinical or prior diagnostic information (age, sex, clinical history, location, presence or absence of tumor) was provided to the pathologist in aiding diagnosis.

Results: Primary neoplasms,margins of surgical resections and lymph nodes specimens to exclude adenocarcinoma, were the common FS specimens. The concordance between G-FS and WSI-FS among pathologists A, B, C, D and E ranged from 90-98%. See Table.

Total Specimens (n)	172					
Pathologists: A,B,C,D and E	G-FS	WSI-FS (A)	WSI-FS (B)	WSI-FS (C)	WSI-FS (D)	WSI-FS (E)
Positive for Adeno Ca	119	119/122 (97%)	122/122 (100%)	111/117 (95%)	111/122 (91%)	113/122 (93%)
Negative for Adeno Ca	50	46/50 (92%)	47/50 (94%)	48/50 (96%)	43/50 (86%)	47/50 (94%)
Suspicious for Adeno Ca	3	0	0	5	0	0
Overall Concordance		165/172 (96%)	169/172 (98%)	164/172 (95%)	154/172 (90%)	160/172 (93%)
p value		0	0	0	0	0
LN Metastasis Concordance	17/172	16/17 (94%)	17/17 (100%)	15/17 (88%)	16/17 (94%)	15/17 (88%)

Conclusions: The concordance between G-FS and WSI-FS interpretations was high. Adenocarcinoma FS diagnosis by WSI is accurate and reproducible. We established diagnostic concordance between digital and glass slides by CAP-PLQC recommended guidelines. This study is the first to specifically evaluate WSI review by specific histopathology subtype.

1577 Implementation of Whole-Slide Imaging in the Routine Diagnosis in a Pathology Laboratory: Consequences for File Storage

Jose Ramirez, Adela Saco, Monica Hernandez, Rosana Millan, Margarita Mainar, Paola Castillo, Natalia Rakislova, Jaume Ordi. Hospital Clinic - Barcelona University, Barcelona, Spain; ISGlobal, Barcelona, Spain.

Background: A major concern about the introduction of whole slide imaging (WSI) in routine diagnosis is the server needs for file storage and its associated costs. We aimed to determine the consequences for file storage of the implementation of this technology in the routine practice of a large hospital.

Design: We conducted the study at the Department of Pathology of the Hospital Clinic of Barcelona, a tertiary, university hospital in Spain. The slides were digitized in a Ventana iScan HT (Roche Diagnostics) at 200x, except for liver and skin pathology, which are digitized at 400x. We evaluated the size of the files generated in the digitalization process over a period of 11 weeks (July-September 2015). We analyzed the increase in terms of file size that scanning at 400x represents over scanning at 200x in a series of 200 glass slides scanned in parallel at these two magnifications. Finally, we calculated the consequences for file storage in terms of the total weight of the files per year.

Results: The number of glass slides scanned during the study period was 8,624. This accounted for 28.8% of the whole activity of the department (29,904 slides in the study period, 141,300 per year). 64.8% of the slides (5,477/8,624) were scanned at 200x and 35.2% (2,972/8,623) at 400x. The size of a single file ranged from 11.5 MB to 6.64 GB, with the mean file size (± standard deviation) being 732.26 ± 710.48 MB. The percentage of images weighing more than 500MB was 52.6% (4,535 out of 8,624); 20.1% images (1,815 out of 8,624) weighed over 1 GB. The size of all the 8,624 files was 6.02 TB bytes. The mean size of a file scanned at 200x was 359.0 ± 273.7 MB, whereas that of the same file scanned at 400x was 1.64 ± 1.04 GB. Thus, scanning at 400x increased the size of the files 4.7-fold. Assuming the same scanning conditions and percentage of slides scanned at 400x for all specimens generated in the study period at the department would have resulted in 20.9 TB, requiring storage needs per year of 98.8 TB.

Conclusions: Theintroduction of WSI in routine diagnosis has a major impact in terms of server needs for storage of the files generated. Scanning at 400x produces a highly significant increase in file size. Strategies to reduce the size of the files and/or to eliminate non-relevant images after a safety period should be developed.

1578 Data Analysis of RNA-Seq of the Bone Marrow from Patients with Myeloid Neoplasms Using Multiple Bioinformatic Pipelines

Thomas Schneider, Geoffrey Smith, Scott Newman, Linsheng Zhang. Emory University, Atlanta, GA; Winship Cancer Institute of Emory University, Atlanta, GA.

Background: RNA-Seq may provide critical information for patients with myeloid neoplasms which frequently involve gene fusions and abnormalities in epigenetic regulations. Bioinformatics alone can be difficult when bringing RNA-Seq into the clinical laboratory. We sought to analyze RNA-seq data generated from bone marrow of myeloid neoplasms with different bioinformatics tools.

Design: RNA from 10 bone marrow samples of myeloid neoplasms were extracted and sequenced on an Illumina HiSeq using Illumina's TruSeq RNA Access (RA). Four samples were sequenced on an Illumina MiSeq using an Agilent SureSelect kit custom-designed to target 44 genes reportedly associated with myeloid neoplasms. Reads were aligned by STAR and Tophat using Varscan for variant calling. RNA expression was generated using Cufflinks and Kallisto. Fusions were queried using STAR-fusion and JAFFA.

Results: Exonic nonsynonymous single nucleotide variants, insertions and deletions with an allele frequency >3%, variant read >2, and minor allele frequency <1% were filtered in. In the RA data set, STAR reported 12,701 variants compared to 489,226 variants by Tophat. Only 4697 variants were common to both aligners and 111 variants were in genes associated with myeloid neoplasms, in which 43 were in the COSMIC database. Significant variants include two *NRAS* mutations, one *IDH2* mutation, two *DNMT3A* mutations, two *TP53* mutations and one *U2AF1* mutation. In comparison, the SureSelect panel identified 81 variants common to both pipelines, with 9 variants reported in COSMIC, including *KRAS* and *SF3B1* mutations. In the RA dataset, 4756 potential fusions were called, yet only 474 by both pipelines and none had junction reads >5 in both pipelines. In contrast, the confirmed *PML-RARA* fusion in the SureSelect dataset was identified by both fusion pipelines with >100 junction reads in both pipelines. Four genes (*DDX5, MPO, DNMT3A, EIF1*) were selected for verification of the relative gene expression levels by real time polymerase chain reaction. Expression levels were concordant except for *EIF1*.

Conclusions: RNA-Seq demonstrated utility in myeloid neoplasms by identifying variants, gene fusions and comparing expressions of different genes. Open source bioinformatic packages for analysis of expression and fusion leave much to be desired. Different pipelines can demonstrate vastly different results in RNA-Seq. Clinically significant variants and fusions need to be verified by alternative methods.

1579 An Enterprise Approach for Pathology Reporting Utilizing PDF Functionality for the Electronic Medical Record

S Joseph Sirintrapun, Tianhao Zhao, Evangelos Stamelos, George Tsividakis, Jonathan Gurman, Mary J Mitchell, Victor E Reuter, David Klimstra. Memorial Sloan Kettering Cancer Center, New York City, NY; Wake Forest Baptist Health, Winston Salem, NC.

Background: Shortcomings are widely known for plain text renderings of pathology reports in electronic medical records(EMRs).With increasing complexity of pathology reports,instead of long narrative text strings,a flexible solution includes Portable Document Format(PDF) renderings of reports.From 3/2014,our group has successfully implemented an architecture for PDF functionality for EMR pathology report integration.

Design: Figure 1 diagrams the architectural framework.

Figure 1

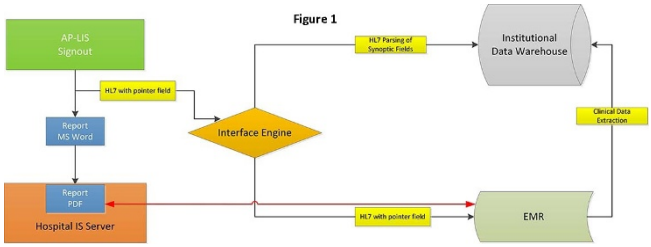

Crucial importance is maintenance of the HL7 feed for data extraction into the institutional data warehouse(IDW).The EMR still maintains the HL7 messaged rendering of the report,to enable copy pasting into clinical documents.

Results: PDF display within the EMR of pathology reports has become primary means by which pathology reports are reviewed.Figure 2 shows #of PDF reports sent across the interface from 3/2014 to 5/2015 which includes a total of 191868 reports,ranging from 11449 to 14422 reports per month with an median & average of 12419 & 12791 reports respectively.

Figure 2

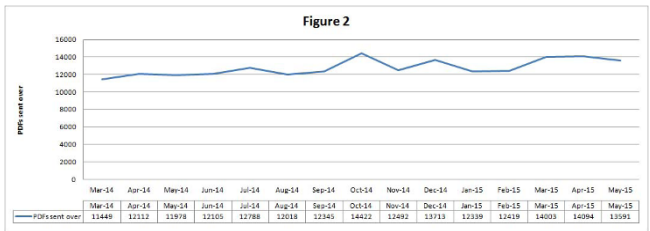

PDF has been highly successful with reports like hematopathology & molecular where complete blood counts & gene mutation lists were improperly laid out under old HL7 plain text renderings in the EMR.

Conclusions: Response has been overwhelmingly positive since pathology report layouts are more intuitive,without constraints of long narrative plain text.Errors in conveying information that occur through formatting are obviated & we have flexibility of colors,bolds,& fonts.Visual analytics is also possible to enable better conveying of information.Many EMR vendors have capability of PDF display & thus we hope our experience can serve as a framework for PDF functionality in EMRs.

1580 Robotic Telecytology for Successful Remote Cytologic Evaluation without On-Site Cytopathology Staffing

S Joseph Sirintrapun, Dorota Rudomina, Rusmir Feratovic, William Alago, Robert Siegelbaum, Oscar Lin. Memorial Sloan Kettering Cancer Center, New York City, NY.

Background: Opening of a remote satellite center in 10/2014 came interventional radiology procedures for cancer diagnoses;some accompanied by FNA & core biopsies mandating rapid on-site cytologic evaluation of smears & biopsy touch imprints for cellular content & adequacy.The volume & frequency of such evaluation did not justify hiring cytotechnologists on-site.Hence a multidisciplinary process re-evaluation along with dynamic robotic telecytology(TC) solution was created.

Design: Sakura VisionTek(SkVT) was selected as our robotic TC solution.Its interchangeable objectives & robotic stage allow for microscopic navigation & magnification in real time.Image viewing & control are remote on HD monitors on main campus via the intranet.The radiology team prepares the cytologic specimen & loads the SkVT.A retrospective analysis was performed of all TC evaluations from this satellite site from 10/2014 to 8/2015.Information was collected on demographics,lesion location,imaging modality,along with comparison of TC assisted adequacy with final adequacy.

Results: Table1 shows demographics,lesion location,& imaging modality.

TABLE1	
TC cases(n=137)	
Demographics	
#patients	137
Mean age(range)	61(18-93)
Sex(male/female)	49/88
Lesion location	
Abdomen	8(5.9%)
Bone	22(16.1%)
Kidney	4(3.0%)
Liver	29(21.2%)
Lymph node	27(19.7%)
Retroperitoneum	12(8.6%)
Soft tissue	35(25.5%)
Image modality	
Ultrasound guided	69
CT guided	68

Table2 compares TC adequacy & final adequacy.

TABLE2			
Comparison of TC assisted adequacy with final adequacy			
	Final Adequacy		Total
TC assisted adequacy	Adequate	Inadequate	
Adequate	116	1	117
Inadequate	7	13	20
Total	123	14	137

Perfect correlation was achieved in 94.1%(129/137) of the cases.Adequacy upgrade(inadequate specimen becomes adequate) was 5.1%(7/137) & adequacy downgrade(adequate specimen becomes insufficient) was 0.7%(1/137).

Conclusions: With radiologic cooperation,dynamic robotic TC was effective for on-site evaluations when cytopathology staff cannot physically be present.Our TC implementation shows high perfect concordance.Adequacy upgrades are minor but not unexpected since only part of material is available during initial review.Most relevant is a near zero adequacy downgrade.Our full implementation has been so successful that plans are in place for future implementations at more satellite sites.

1581 Successful Secure HD Streaming Telecytology for Remote Cytologic Evaluation

S Joseph Sirintrapun, Dorota Rudomina, Rusmir Feratovic, Oscar Lin. Memorial Sloan Kettering Cancer Center, New York City, NY.

Background: Because of expansion of numerous remote stationary locations whereby a cytotechnologist was available but an attending pathologist for on-site evaluation was not possible physically,a process re-evaluation along with streaming telecytology(TC) solution was created.Since 6/2015,cellular content & adequacy were affirmed through TC for fine-needle aspiration(FNA) smears & touch imprints of core biopsies(CBs).

Design: Remote Medical Technologies(RMT) was selected as a highly secure dynamic streaming TC solution.A linux server coordinates broadcast of live images captured through HD cameras connected to routing devices which then communicate with the linux server securely over the intranet.The cytology attending at a central location can then view live images seamlessly on HD monitors,through secure authentication mechanisms on the system backend.We performed retrospective analysis of all remote TC evaluations for FNA & touch preps of CBs from 7/2015 to 8/2015.Information was collected on demographics,body site,along with a comparison of TC assisted adequacy with final adequacy assessment.

Results: Table 1 shows case breakdown per remote location,demographics,& body site.

TABLE1	
TC cases(n=431)	
Remote Locations	
Location1	240
Location2	153
Location3	38
Demographics	
#patients	390
Mean age(range)	62(6-98)
Sex(male/female)	1.1/1
Body site	
Lung	86
Liver	66
Lymph node	55
Bone	46
Soft tissue	30
Thyroid	25
Other	82

Table 2 shows an adequacy comparison between the TC adequacy assessment & the final adequacy.Perfect concordance was 92.6%(399/431).Adequacy upgrade (inadequate specimen becomes adequate) was 7.2%(31/431) and adequacy downgrade(adequate specimen becomes insufficient) was 0.2%(1/431).

TABLE2			
Comparison TC assisted adequacy with final adequacy			
TC assisted adequacy	Final adequacy		Total
	Adequate	Inadequate	
Adequate	353	1	354
Inadequate	31	46	77
Total	384	47	431

Conclusions: Strengths are security & authentication mechanisms,along with usability/seamless integration into workflow.Image quality & speed are excellent. Despite interruption to view a TC assessment,disruption which occurs with figuring setup with Web-Ex or Go to Meeting is obviated.Our implementation shows high perfect concordance.Adequacy upgrades are minor but not unexpected since only part of material is available during initial review.Most relevant is a near zero adequacy downgrade.Our implementation has been successful that plans are to extend TC on mobile carts.

1582 Multi-Site Digital Pathology Validation Using Standardized Coded Checklists and Predetermined Discordance Tables

Katy Wack, Laura M Drogowski, Murray Treloar, Andrew Evans, Jonhan Ho, Anil Parwani, Michael Montalto. Omnyx, LLC, Pittsburgh, PA; Dr. Murray Treloar Medicine Professional Corp, Port Hope, ON, Canada; University Health System, Toronto, ON, Canada; University of Pittsburgh Medical Center, Pittsburgh, PA; Ohio State University Wexner Medical Center, Columbus, OH.

Background: Manual arbitration between paired diagnoses is a labor intensive process that does not allow for consistent, scalable and repeatable data. The purpose of this study was to pilot a novel method of data capture and analysis using standardized codified CAP checklists and predetermined synoptic discordance tables. We used this method to pilot a scalable, multi-site validation of whole slide images (WSI) for the purpose of primary diagnosis.

Design: Discordance tables were generated by making pair-wise comparisons between every possible diagnostic response from 44 CAP cancer protocols. Thousands of discrete paired entries for this study were evaluated and each theoretical discordance was assigned a level harm.

The cases in the pilot WSI validation study were enriched for challenging, atypical or malignant diagnoses, spanning 8 organ systems and multiple procedure types. Cases were scanned on a conventional WSI scanner at 40x (0.275 µm/pixel). 16 pathologists, 4 at each of 4 sites, each read 8 cases with a two-week wash-out between glass and WSI reads. Data from all readers was pooled for a total of 132 paired diagnoses to be evaluated for intra-reader/intra-modality comparison to ground truth (original sign-out diagnosis), and 178 paired evaluations for intra-modality/inter-reader.

Results: The average error rate for glass across all readers was 12.1 % (16 major discordances out of 132 comparisons) and 11.4% (15 major discordances out of 132 comparisons) for WSI. Major discordances occurred on challenging cases, regardless of modality (i.e., small focus of ADH in a breast biopsy). The average difference in error rate between WSI and glass was 0.75% with a lower bound of 3.23% (95% CI). The average inter-reader agreement across sites for glass was 76.5% (weight kappa of 0.68) and for digital was 79.1% (weighted kappa of 0.72) with no significant difference between modalities.

Conclusions: These results demonstrate the feasibility and utility of employing standardized synoptic checklists and discordance tables to gather consistent, comprehensive diagnostic data for WSI validation studies. This method of data capture and analysis should be applicable in validation, quality, and other studies measuring the impact of any intervention on pathology diagnoses.

1583 Computer Extracted Features of Nuclear Morphology from Digital H&E Images Are Predictive of Recurrence in Stage I and II Non-Small Cell Lung Cancer

Xiangxue Wang, Andrew Janowczyk, Yu Zhou, Sagar Rakshit, Vamsidhar Velcheti, Anant Madabhushi. Case Western Reserve University, Cleveland, OH; Cleveland Clinic, Cleveland, OH.

Background: Approximately 80% of all lung cancers are non-small cell lung cancers (NSCLC), making it the leading cause of cancer related deaths around the world. While most early stage NSCLC respond favorably to treatment, a subset of patients will experience recurrence. The ability to identify which early stage NSCLC will recur can help modulate therapy, while more aggressive therapies can be employed for patients identified with a higher risk of recurrence. Currently pathologists have no way of predicting disease recurrence by inspecting H&E images of lung biopsy specimens alone. In this study, we show that computer extracted features of nuclear morphology from digital H&E images of lung biopsies are predictive of recurrence in Stage I and II NSCLC.

Design: The dataset used in this study consists of 2 tissue microarrays (YTMA79, n = 69 and YTMA140, n = 46), where YTMA140 was used for learning the most discriminating image based features and YTMA79 was used for independent validation. The image analysis pipeline consists of nuclei detection and segmentation, followed by nuclei based feature extraction, feature selection, classification and survival analysis.

Results: A deep learning approach was used to identify nuclei. The Haralick texture (Fig. 1(c-d)) and shape descriptors (Median Fractal Dimension) of nuclei were found

to be the most predictive in distinguishing between early stage NSCLC (Fig. 1(a-b)) recurrence from non-recurrence patients. A random forest classifier trained with Haralick and shape features yielded a 0.78 AUC on YTMA140, using 2/3 for training and 1/3 for validation over 100 repeated random sub-sampling and (Fig. 1(e)) 0.71 on YTMA79. Survival predictions for these 2 groups of patients was shown to be statistically different with p-value 0.02 (Fig. 1(f)).

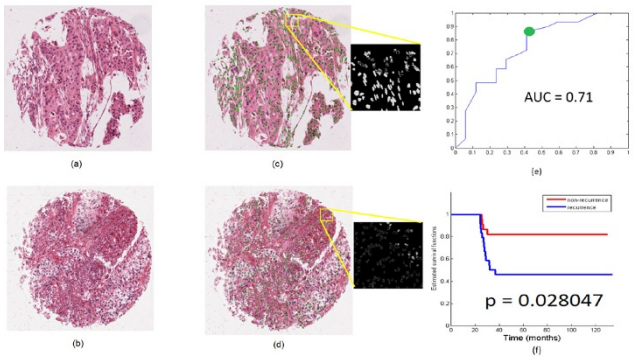

Figure 1: Sample TMA of (a) non-recurrence and (b) recurrence NSCLC. Haralick texture (standard deviation intensity correlation) feature of nuclei on (c) non-recurrence and (d) recurrence NSCLC show obvious intensity difference. (e) Receiver operating characteristic plot with operating point highlighted and (f) Kaplan-Meier curves generated via the random forest classifier.

Conclusions: We found that a combination of computer extracted nuclear texture and shape features could potentially be used to identify recurrence in early stage NSCLC. These features were found to yield a statistically significant difference in likelihood of recurrence between patients in both training and independent validation cohorts.

1584 Central Histopathology Review of Essential Thrombocythemia and Polycythemia Vera Bone Marrow Biopsies via Digital Tools in a Clinical Trial on Pegylated Interferon Alfa-2a

Delu Zhou, Olga Pozdnyakova, Rajan Dewar, Robert P Hasserjian, Ali Etman, Ronald Hoffman, Mohamed E Salama. University of Utah, Salt Lake City, UT; Brigham and Women's Hospital, Boston, MA; University of Michigan, Ann Arbor, MI; Massachusetts General Hospital, Boston, MA; Mount Sinai School of Medicine, New York, NY.

Background: Central pathology review for clinical trials often require specimen examination by pathologists from geographically separated institutions. This study is designed to explore the possibility of utilizing whole slide digital imaging (WSI) and computer-assisted image technology (CAI) to facilitate the central review process in a clinical study of polycythemia vera (PV) and essential thrombocythemia (ET) sponsored by MPD Research Consortium (MPD-RC). We report here interval pathology review findings.

Design: Cases of PV and ET patients treated with Pegylated Interferon Alfa-2a from MPD-RC clinical trial were studied. The bone marrow (BM) core biopsy H&E and reticulin slides from samples collected before and after treatment were scanned with Aperio AT-2 scanner. E-slide management system was used to provide remote access to images. Cytonuclear algorithm of HALO imaging software was used to quantify bone/hematopoietic area and cellularity. 55 samples were reviewed by at least two hematopathologists from separate institutions according to predefined criteria. 95 specimens were evaluated by CAI.

Results: Pathologists were able to successfully perform morphological evaluation via digitalized central review process. The analysis showed high agreement rate on megakaryocyte size (94%) and clustering (72%), osteosclerosis score (88%), fibrosis score (74%) , cellularity (81%) and lymphoid aggregates (88%), but low agreement for megakaryocytes nuclear lobulation (36%) and dysplasia (40%) and erythroid quantification (40%). 5/6 patients showed significant decrease in trabecular bone areaas associated with increase in fat at 24 months post-treatmentas. CAI also showed higher correlation with the average cellularity identified by direct visualization (correlation coefficient is 0.88), when compared to interobserver correlation of visual cellularity estimated by different pathologists (correlation coefficient is 0.81). PV cases showed higher cellularity relative to ET cases at baseline (p=0.0043) or post-treatment samples (p=0.029).

Conclusions: WSI is a feasible and useful tool for central pathology review in clinical trials. CAI provided added value to morphology for more objective evaluation of BM histology. High concordance can be achieved with defined criteria for histotopography evaluation.

Kidney/Renal Pathology (including Transplantation)

1585 mRNA Diagnosis of Antibody-Mediated Rejection from Routine Paraffin Sections of Renal Transplant Biopsies in a Nonhuman Primate Model

Benjamin Adam, R Neal Smith, Tatsuo Kawai, A Benedict Cosimi, Robert B Colvin, Michael Mengel. University of Alberta, Edmonton, AB, Canada; Harvard Medical School and Massachusetts General Hospital, Boston, MA.

Background: In 2013, the Banff classification proposed molecular diagnostics as an adjunct for the diagnosis of antibody-mediated rejection (ABMR) in renal allografts. To catalyze clinical adoption of this approach, we tested whether mRNA from formalin-fixed paraffin-embedded (FFPE) tissue samples could be analyzed with the new NanoString nCounter gene expression platform, using archival tissue blocks from serial protocol biopsies of nonhuman primates that developed chronic ABMR.

Design: 34 genes (endothelial, NK cell, inflammatory) previously associated with ABMR in humans were compiled into a monkey specific NanoString nCounter probe set. RNA was isolated from 56 FFPE sections (3 x 20 µm) including 48 sequential renal allograft biopsies from 12 Cynomolgus monkeys that developed ABMR after tolerance induction protocols without specific ABMR treatment (Smith et al Am J Transplant 8:1662, 2008) and compared with 8 normal kidney controls. Gene set expression was quantified and correlated with histology, C4d, and serology.

Results: Gene set expression was significantly higher in biopsies with histologic diagnoses of ABMR compared with normal controls (p=0.00007). It was also higher in C4d positive vs. negative (p=0.000007) and donor specific antibody (DSA) positive vs. negative (p=0.0006) biopsies. Some animals (e.g. 5198, 6000) exhibited increasing gene set expression with histologic ABMR progression. Other animals (e.g. 1902, 6007) demonstrated stable or decreasing expression with histologically persisting ABMR. Biopsies with histologic diagnoses of TCMR showed increased ABMR gene set expression before developing histologic evidence of ABMR, suggesting that molecular testing is predictive and more sensitive than histology for early ABMR.

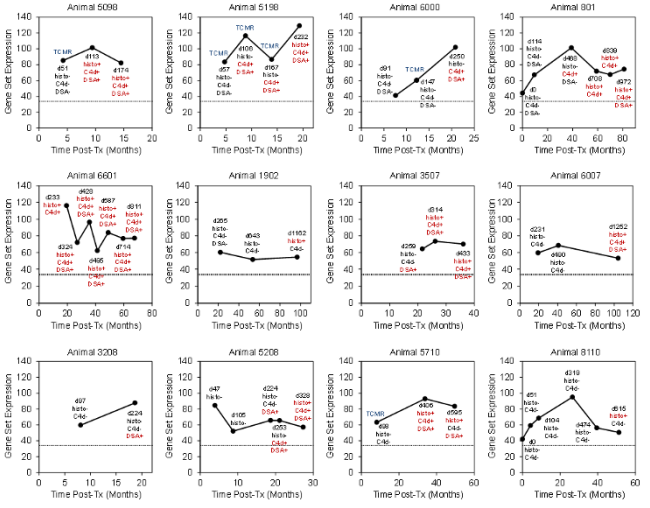

[1]Gene set expression = geometric mean of normalized NanoString counts.
[2]Dashed line = mean gene set expression in normal controls (2+SE).
[3]Histologic categories: normal/other/borderline/TCMR = 'histo-', ABMR/mixed rejection = 'histo+'.
[4]ABMR, antibody-mediated rejection; DSA, donor specific antibodies, TCMR, T-cell mediated rejection.

Conclusions: Robust multiplexed gene expression quantification from nonhuman primate FFPE renal allograft biopsies is feasible using the NanoString platform. Preliminary animal model validation indicates significant potential for a set of endothelial, NK cell, and inflammatory transcripts in diagnosing ABMR and assessing disease activity.

1586 Acute Allograft Glomerulopathy: A Distinct Form of Cellular Rejection

Osamah AL-Badri, Mariam P Alexander, Fernando G Cosio, Lynn D Cornell. Mayo Clinic, Rochester, MN.

Background: Acute allograft glomerulopathy (AAG) is a glomerular lesion of renal allografts characterized by endocapillary hypercellularity with mononuclear cell infiltration and markedly enlarged endothelial cells occluding the capillary lumen, and absence of immune complex deposits. AAG is not currently a rejection lesion recognized by the Banff schema.

Design: We searched a database for biopsies that showed AAG. Light microscopy slides and C4d staining status were reviewed, as were follow-up biopsies. Treatment and clinical follow up data were obtained.

Results: We identified 15 patients with AAG in renal allograft biopsies from Jan 2009 through Aug 2015, accounting for <1% of biopsies showing rejection during this time period. The mean patient age was 56.4 years (range 22-76); ~54% of transplants were from living donors. The mean time post-transplant was 3.2 months (range 0.1 to 11). The biopsy indication in 14 was increased serum creatinine (SCr), mean 3.2 mg/dl (range 1.5-9.4); one was a 4 month protocol biopsy.

All biopsies showed glomerulitis by definition. In addition, the glomeruli showed focal segmental to global marked endothelial enlargement with occlusion of the capillary lumens and infiltrating mononuclear cells and neutrophils. No GBM duplication was present. 12/15 (80%) showed arteritis (Banff v lesions), including 4 with v2 or v3 lesions. 8/15 (53%) showed mild or no interstitial inflammation; 9/15 (60%) showed mild or no tubulitis. 14/15 (93%) were C4d negative; one showed focal C4d PTC staining. 2 showed moderate peritubular capillaritis. 3/15 (20%) showed focal thrombi in vessels or mesangiolysis. Immunofluorescence was negative for immune complexes in all.

6/12 (50%) of patients with data available had a history of donor-specific antibody. 9 patients were on triple immunosuppression. Treatment information was available in 10 patients; all were treated with immunosuppression (anti-thymocyte globulin in 5 and steroid bolus in 5). Up to 1 year after the biopsy showing AAG, the SCr decreased in 9/13 (69%) patients alive with data available, mean 1.7 mg/dl (range 0.9-3.3). Follow up biopsies were performed in 7 patients; 5 of these (71%) showed continued AAG lesions.

Conclusions: AAG is a rare but distinct histopathologic lesion that is highly correlated with vascular rejection and rarely accompanied